

# MECHANICAL BEHAVIOR OF THERMOMECHANICALLY PROCESSED $\beta$ TITANIUM ALLOY – TITANIUM ALUMINIDE LAMINATE COMPOSITE

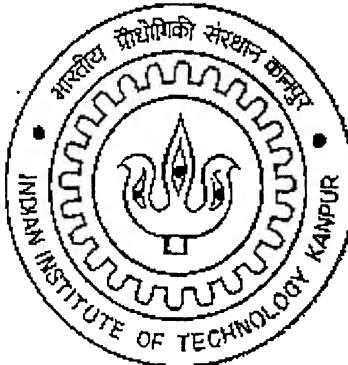
*A Thesis Submitted*

In Partial Fulfillment of the Requirements  
For the Degree of

**MASTER OF TECHNOLOGY**

by

**Girjesh Shukla**  
(Roll No. Y010612)



*to the*

**DEPARTMENT OF MATERIALS AND METALLURGICAL ENGINEERING  
INDIAN INSTITUTE OF TECHNOLOGY, KANPUR**

May, 2002

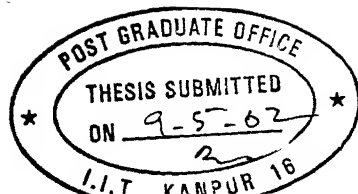
4 FEB 2003 /MME

पुरुषोत्तम काशीनाथ केवकर पुस्तकालय  
भारतीय बौद्धोगिकी संस्थान कानपुर

अवाप्ति क्र. A 141916



A141916



## CERTIFICATE

This is to certify that the thesis entitled "**Mechanical Behavior of T  
processed  $\beta$  Titanium Alloy -Titanium Aluminide Laminate Co  
Shukla (Roll No. Y010612)**", has been carried out under my supervis  
my knowledge this work has not been submitted elsewhere for a degre

Department of Materials and Meta  
Indian In  
K

May 2002

## Acknowledgments

With a profound sense of gratitude, I express my sincere thanks to my thesis supervisor Dr. Sanjeev Bhargava for his invaluable guidance. I am really grateful for his encouragement throughout the work and for providing me all the facilities and help in every possible way at IIT- Kanpur.

I gratefully acknowledge the unconditional help received from Mr. Amit Bhattacharjee, DMRL Hyderabad during my thesis work. I am also grateful to Dr. Mungole, Mr. Surendra, Mr. Kumar, Mr. Jain, Mr. Rajan and Mr. Chandrashekhar for their help during my experimental work.

I would also like to mention the name of my friends Dr. Dilip, Barun and Navin, who always supported me particularly in difficult time. I would also like to acknowledge the love and affection given by my family without which I would not have come to this stage.

At last but not the least I would also like to acknowledge thanks to my friends Vineet(Azhar), Jangid, Rajneesh , John, Shyam, Tyagi , Gautam, Amit, Aditya, Shankar and laha who have helped me throughout the experimental work.

Girjesh Shukla  
IIT, Kanpur.

## ABSTRACT

Metallic - Intermetallic laminate composite having  $\beta$  Titanium alloy Ti-10 V- 4.5 Fe - 2 Al (the metallic phase) and titanium aluminide Ti-22 Al- 25 Nb- 0.5 Mo (the intermetallic phase), prepared via hot pressing route and comprising of twelve alternate layers of 1mm thick sheets of the two constituents have been subjected to different thermomechanical processing via hot as well as warm rolling route. Hot rolling behaviour of the laminate composite at temperatures above the  $\beta$ -transus temperature of the metallic phase and below the transus temperature of the intermetallic phase shows that the laminate composite could be hot rolled up to about 10% to 15% thickness reduction in a single pass without any edge and/or surface cracking. Microstructures of hot rolled samples show elongated  $\beta$  grains in the metallic phase indicating that no dynamic recrystallization takes place in metallic phase. In contrast, the intermetallic phase shows the presence of fine equiaxed grains. Warm rolling at  $700^0\text{C}$ , i.e. below the  $\beta$ -transus temperature of the metallic phase, could be done with low values of % thickness reduction in a single pass. Annealing behaviour of the laminate composite showed that annealing above  $\beta$  transus of the  $\beta$  alloy results into coarse  $\beta$  grains in the metallic phase. In contrast, annealing at temperatures below the  $\beta$  transus of the metallic phase, i.e. at  $550^0\text{C}$ ,  $600^0\text{C}$ ,  $650^0\text{C}$  and  $700^0\text{C}$ , for sufficiently long time intervals results in the precipitation of fine  $\alpha$  grains in  $\beta$  alloy layer of the composite. Room temperature tensile properties of the laminate composite depended on the hot rolling temperature. For the samples rolled at  $950^0\text{C}$ , the yield strength has been found to be  $> 1150$  MPa which is roughly equal to that predicted by the rule of mixtures for the laminate composites. UTS of the composite rolled at this temperature is found to be  $> 1190$  MPa. The composite is also more ductile, having about 9% elongation, than that reported in the literature. While the yield strength and the UTS of the laminate composite deteriorate when the hot rolling temperature is increased above  $950^0\text{C}$ , the ductility increases. An annealing treatment of 24 hours at  $550^0\text{C}$  deteriorates the yield strength as well as the ductility of the laminate composite rolled at  $950^0\text{C}$  and  $1000^0\text{C}$ . However, this treatment increases the ultimate tensile strength of the material. Laminate composites subjected to warm rolling at temperatures below the  $\beta$ -transus temperature of the metallic phase display inferior tensile properties. Warm rolling of the laminate composites therefore is not recommended.

# CONTENTS

<b>TABLE OF CONTENTS</b>	i
<b>LIST OF FIGURES</b>	iii
<b>LIST OF TABLES</b>	v
<b>Chapter 1. INTRODUCTION</b>	1
<b>Chapter 2 LITERATURE REVIEW</b>	3
2.1 Titanium and its alloys	3
2.2 Important physical properties	3
2.3 Classification of Titanium alloys	8
2.3.1 $\alpha$ Titanium alloys	11
2.3.2 Near $\alpha$ Titanium alloys	11
2.3.3 $\alpha + \beta$ Titanium alloys	12
2.3.4 Near- $\beta$ Titanium alloys	12
2.3.5 $\beta$ Titanium alloys	13
2.4 Microstructural features of titanium alloys	13
2.5 Laminate Metal Composites	19
2.5.1 Formation of laminates	19
2.5.2 Bonded Laminates	19
2.5.3 Deformation response of Laminate during bonding	20
2.5.4 Tensile behavior of laminate composite	21
<b>Chapter 3. EXPERIMENTAL PROCEDURE</b>	28
3.1 Material for the present investigation	28
3.2 Thermo-mechanical treatment	30
3.2.1 Hot rolling	30
3.2.2 Warm rolling	30

3.3	Microstructural characterization	32
3.3.1	Sample preparation & optical microscopy	32
3.3.2	Quantitative microscopy	32
3.4	Mechanical testing of the sample	33
3.4.1	Microhardness Testing of the Samples	33
3.4.2	Tensile Testing of the Samples	33
<b>Chapter 4. RESULT AND DISCUSSIONS</b>		<b>35</b>
4.1	Rolling Behavior of Laminate Composite	35
4.1.1	Hot Rolling Behavior of Laminate Composite	35
4.1.2	Warm Rolling Behavior of Laminate composite	37
4.2	Annealing behavior of rolled laminate composite	38
4.2.1	Annealing of composite material rolled at 950 <sup>0</sup> C	38
4.2.2	Annealing of composite material rolled at 1000 <sup>0</sup> C	44
4.2.3	Annealing of composite material rolled at 1050 <sup>0</sup> C	48
4.3	Mechanical behavior of thermomechanically treated laminate composite	53
4.3.1	Effect of thermomechanical/ annealing treatment on microhardness of $\beta$ phase and aluminide phase	53
4.3.2	Tensile behavior of thermomechanically treated laminate composite	60
4.3.2.1	Tensile behavior at high temperature	60
4.3.2.2	Tensile behavior at room temperature	60
<b>Chapter 5. CONCLUSIONS</b>		<b>67</b>
<b>SUGGESTIONS FOR FUTURE WORK</b>		<b>69</b>
<b>REFERENCES</b>		<b>70</b>

## LIST OF FIGURES

### Figure

2.1.	Crystal structure of titanium	5
2.2.	Schematic diagrams of binary titanium alloy system	10
2.3.	Tools made by laminated metal composite	23
2.4.	Deformation response of the laminate during press bonding	24
2.5.	Breaking strength of ultra thin layer laminated composites as a function of modulating spacing.	25
2.6	Experimental yield strength of a thick layer laminated composite	26
2.7	Experimental tensile elongation to fracture curve	27
3.1	As received sample (a) Aluminide phase (b) $\beta$ alloy phase (c) shape and dimensions of as received sample.	29
3.2	Process flow diagram	31
3.3	Dimensions of Tensile Testing Specimen	34
4.1	Microstructures of the sample hot rolled at (a) 950°C (b) 1000°C (c) 1050°C with 30%deformation (d) 1050°C with 83% deformation	36
4.2	Microstructures of (a)Aluminide phase and (b) $\beta$ Alloy phase hot rolled at 950°C	39
4.3	Microstructure of the sample hot rolled at 1000°C and subsequently warm rolled at 700°C	40
4.4	Microstructure of the sample hot rolled at 950°C and annealed for 30 minutes at (a) 650°C (b) 750°C (c) 750°C and (d) 800°C	41
4.5	Microstructures of the sample hot rolled at 950°C and annealed at 700°C for (a) 70 min (b) 20 hrs (c) 30 hrs.	42
4.6	Microstructure sample hot rolled at 950°C and heat treated at 650°C for 45 hrs	43
4.7	Sample hot rolled at 1000°C and annealed for 30 minutes for (a) 650°C (b) 700°C (c) 750°C (d) 800°C	45
4.8	Microstructures of the sample hot rolled at 1000°C / warm rolled at 700°C and annealed at 700°C for (a) 2 hrs (b) 20 hrs.	46

4.9	Microstructures of sample hot rolled at 1000 $^0\text{C}$ and warm rolled at 700 $^0\text{C}$ and annealed at 550 $^0\text{C}$ for (a)24 hrs (b) 48 hrs (c) 72 hrs.	47
4.10	Microstructures of the sample hot rolled at 1050 $^0\text{C}$ and annealed at 550 $^0\text{C}$ for (a) 3 hrs (b) 12 hrs (c) 18 hrs.	49
4.11	Microstructures of the sample hot rolled at 1050 $^0\text{C}$ and annealed at 550 $^0$ for (a) 24 hrs (b) 48 hrs (c) 72 hrs.	50
4.12	Grain size vs. Annealing time curve.	51
4.13	Aspect ratio vs. Annealing time curve.	52
4.14	Microhardness values of (a) Aluminide layer (b) $\beta$ titanium alloy layer as a function of rolling temperature.	54
4.15	Microhardness value as a function of rolling temperature	55
4.16	Microhardness value as a function of annealing temperature for (a)aluminide layer (b) $\beta$ alloy layer	56
4.17	Microhardness value as a function of annealing temperature.	57
4.18	Microhardness value as a function of annealing time (a) Aluminide Layer (b) $\beta$ Alloy layer	58
4.19	Microhardness value as a function of annealing time	59
4.20	Tensile curves at room temperature for the specimens rolled at (a) 950 $^0\text{C}$ (b) 1000 $^0\text{C}$ and (c) 1050 $^0\text{C}$	63
4.21	Room temperature tensile properties for three rolling temperatures (a)% Elongation (b)UTS (c) YS.	64

## LIST OF TABLES

### Table

2.1	Selected physical properties of titanium as compared to those of aluminum and iron	4
2.2	Physical properties of elemental titanium	6
2.3	Classification of U.S. Technical Multi component Alloys	14
2.4	Typical room temperature Tensile Strengths of some commercial titanium based alloys	16
2.5	Comparative properties of some metals	17
2.6	Comparative properties of some alloys	18
3.1.	Chemical composition of the material used in the investigation	28
4.1	Grain size as a function of annealing time for the sample hot rolled at $1050^0\text{C}$ and annealed at $550^0\text{C}$	51
4.2	Aspect ratio as a function of annealing time for the sample hot rolled at $1050^0\text{C}$ and annealed at $550^0\text{C}$	52
4.3	Microhardness values for the two layer at different rolling temperatures	55
4.4	Microhardness values for the two layer as a function of annealing temperatures	57
4.5	Microhardness behavior of composite with annealing time	59
4.6	Strength and Elongation in the sample tested at higher temperature	62
4.7	YS, UTS and Percentage Elongation ( at room temperature) of the samples rolled at three different temperatures.	62
4.8	YS, UTS and Percentage Elongation of the samples rolled at three different temperatures and annealed at $550$ deg C for 24 hrs	65
4.9	Tensile properties of sample hot rolled at $1000^0\text{C}$ , warm rolled at $700^0\text{C}$ and annealed at $550^0\text{C}$ for 24 hours	65
4.9	Mechanical properties of some $\beta$ alloys, intermetallics and laminated composites of titanium alloy	66

# Chapter 1

## INTRODUCTION AND OBJECTIVE

Laminated metal composites are the materials that consist of alternate metal or metal-containing layers bonded together with discrete interfaces. Many mechanical properties such as fracture toughness, fatigue behavior, impact behavior, wear, corrosion, and damping capacity, ductility, formability etc. can be improved using these laminated metal composites. At low temperature, very high tensile strengths can be achieved in roll bonded laminates by layer thickness refinement. At high temperature, superplasticity may be achieved. A wide range of applications such as airframes, thermostats, electronics packaging etc are attributed to such materials. Alternating brittle but creep resistant compositions with tough materials can be of particular interest because the dissimilar properties of the constituents provide an ideal opportunity for achieving the desired property combinations. The most widely known composite of this class is metal ceramic composites. Another suitable composite of this class is composite based on metal-intermetallic combinations.

Metal-intermetallic composites offer an attractive combination of properties from both constituent phases, i.e. high stiffness as well as low density of intermetallics, and the high toughness of metals. Orthorhombic titanium aluminide alloys have excellent high temperature properties which is required in high temperature gas turbine materials. The Intermetallic Titanium Aluminide compounds such as  $Ti_3Al$ ,  $TiAl$ ,  $TiAl_3$  etc based alloys, exhibit high specific strength and good high temperature properties, which make them attractive for hypersonic applications or advanced engines. These exceptional properties result from their ordered microstructure, however, poor formability, low ductility and toughness associated with these intermetallic alloys restricts their applications [1].

In order to come up with the limitations associated with these Intermetallic Titanium Aluminide based alloys, we can try for laminated metal composites. Laminated metal composites are important engineering alloys due to their attractive combination of

properties such as strength, fracture resistance, stiffness, tensile strength, notch strength, creep and fatigue resistance are superior for such layered composites. In the present work, Laminated Composite fabricated using Titanium Aluminide based intermetallic alloys and  $\beta$ - Titanium alloy will be studied. Beta Titanium alloy is having superior room temperature properties while Titanium Aluminide based intermetallic alloy has good high temperature properties [2,3,4]. Laminate composite material in the present study consists of composite sheets of (O+B2) intermetallic alloy and  $\beta$  Titanium alloy (fabricated in the laboratory scale using a two-step process involving diffusion bonding and hot rolling).

The present work deals with determination of hot and warm rolling behavior of the laminate composite, determination of the optimum time/ temperature of heat treatment to obtain a fine structure in the laminate and analysis of mechanical behavior of the laminate composite as a function of rolling temperature and annealing temperature/ time, and high temperature tensile properties of the laminate composite.

# Chapter 2

## LITERATURE REVIEW

### 2.1. Titanium and its Alloys

Interest in the properties of Titanium and its alloys began to accelerate during the late 1940s and early 1950s. Titanium alloys are attractive since they have a high strength to weight ratio, high elevated-temperature properties to about  $550^{\circ}\text{C}$ , and excellent corrosion resistance, particularly in oxidizing acids and chloride media and in most natural environments [5].

Unfortunately, titanium and its alloys cost somewhat more than common metals because they are difficult to extract from their ores and sophisticated melting and fabricating techniques must be used in their manufacture. The higher cost of titanium alloy fabrication is principally the result of metal's high reactivity and affinity for interstitial elements such as oxygen, nitrogen, hydrogen, and carbon. Nevertheless, titanium and its alloys do compete effectively in many areas where their special properties can be used to advantage. For example, high strength-to-weight ratio and high elevated-temperature properties of titanium alloys are of prime importance in the aerospace industry. The excellent corrosion resistance of titanium makes it particularly useful for the chemical and food industries. New uses for titanium and its alloys are being constant sought and discovered.

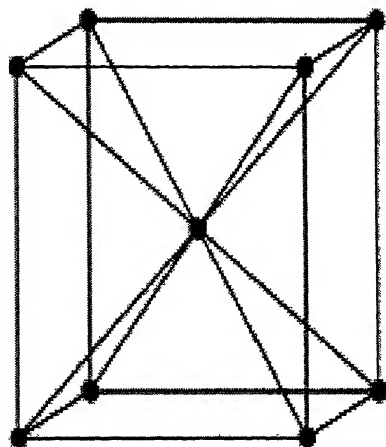
### 2.2 Important physical properties

Titanium is a relatively light metal having a density of  $4.54 \text{ g/cm}^3$ , which is intermediate between that of aluminum ( $2.71 \text{ g/cm}^3$ ) and iron ( $7.87 \text{ g/cm}^3$ ). Titanium has a high melting point of  $1668^{\circ}\text{C}$ , which is higher than that of iron ( $1536^{\circ}\text{C}$ ), and a modulus of elasticity of  $16.8 \times 10^6 \text{ lb/in}^2$ , which is intermediate between the values for aluminum and iron. The density, melting point and modulus of elasticity of titanium are compared with those properties of aluminum and iron. Titanium is paramagnetic in nature and shows a relatively lower coefficient of thermal expansion and high electrical resistivity. Some important physical properties of titanium are shown in table 2.1

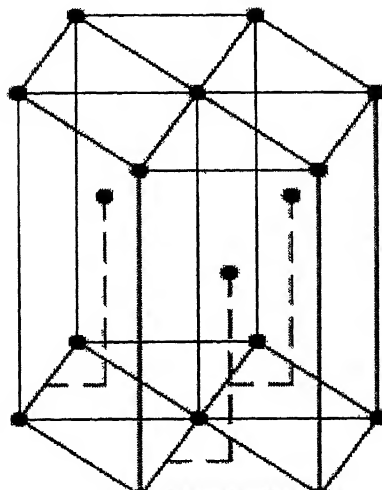
**Table 2.1 Selected physical properties of titanium as compared to those of aluminum and iron**

Property	Titanium	Aluminum	Iron
<b>Density</b> (g/cm <sup>3</sup> )	<b>4.52</b>	<b>2.71</b>	<b>7.87</b>
<b>Modulus of elasticity</b> *10 <sup>6</sup> lb/ in <sup>2</sup>	<b>16.8</b>	<b>9.0</b>	<b>28.5</b>
<b>Melting point</b> °C	<b>1668</b>	<b>660</b>	<b>1536</b>
<b>Crystal structure at room temperature</b>	<b>HCP</b>	<b>FCC</b>	<b>BCC</b>

Titanium exists in two allotropic crystal forms. These are  $\alpha$ , which has the hexagonal close-packed (HCP) structure, and  $\beta$ , which has the BCC crystal structure. In pure titanium, the  $\alpha$  phase is stable up to 883°C. Above 883°C, the  $\beta$  transus temperature, the hexagonal  $\alpha$  phase is transformed on heating to the BCC  $\beta$  phase.



BODY-CENTERED CUBIC



HEXAGONAL  
CLOSE PACKED

Fig 2.1 a-b Crystal structure of Titanium

**Table 2.2 Physical properties of elemental titanium**

Atomic number	22
Atomic weight	47.90
Atomic volume	10.6 W/D
Covalent radius	1.32 Å
First ionization energy	158 K-cal/gm-mole
Thermal neutron absorption cross section	5.6 barn/atom
Colour	dark gray
Melting point	1941±10 K
Solidus/Liquidus	1998±10 K
Boiling point	3533 K
Specific Heat (at 25 °C)	0.518 J/kg K
Thermal Conductivity	9.0 BTU/ hr ft <sup>2</sup> °F
Heat of Fusion	440 kJ/kg
Heat of Evaporation	9.83 MJ/kg
Heat of Transformation	678 cal/mole
Young's Modulus	10.7*10 <sup>11</sup> dyne/cm <sup>2</sup>
Temp. Coefficient of Young's Modulus	6.28*10 <sup>8</sup> dyne/cm <sup>2</sup> °F
Modulus of rigidity	(3.87±0.1)* 10 <sup>11</sup> dyne/cm <sup>2</sup>
Poisson's ratio	0.36
Coefficient of friction	0.8 at 40 m/min
Coefficient of linear expansion	(8.35±0.15)* 10 <sup>-6</sup> /°C at 15 °C
Electrical Resistivity	(42.05±0.5)* 10 <sup>-6</sup> ohm-cm
Magnetic Susceptibility	3.2±0.4 emu/gm
Work Function	4.05± 0.1 eV
Electronic specific heat	8.0±10 <sup>-4</sup> cal/ °C mol

Titanium alloys with strength capability almost equivalent to low carbon steels and density little more than half (about 56%) of that of low carbon steels, can be strengthened to achieve a specific strength (strength per unit weight) equal to that of ultra high strength steels. Titanium approaches the high hardness value possessed by some of the heat-treated alloy steels. Titanium and its alloys have exceptionally high fatigue strength, if the surface is carefully prepared. It is 0.82 and 0.31 of tensile strength for un-notched and notched samples, respectively, and thus lies in the same range as the steels. Fatigue crack growth rate of annealed Ti-6-4 alloy in distilled water are enhanced as compared with that in air; the growth rates are found to decrease with increasing temperature and frequency.

Titanium alloys shows creep at room temperature; creep strength of titanium normally decreases at first, but at  $120^{\circ}\text{C}$  begins to increase again, reaching a maximum at  $200^{\circ}\text{C}$ , thereafter falls gradually with increase in temperature. Cold working of titanium increases its creep resistance at room temperature. The Charpy impact strength dropped from an average of 15 ft-lb at room temperature to about 6 lb-ft at liquid nitrogen temperature. The specific fracture toughness ( $K_{\text{IC}}$  per unit weight) of titanium alloys is superior to most of the structural materials. Table 2.3 & 2.4 compare some mechanical properties of Ti and its alloys with some other metals and alloys.

Corrosion resistance of titanium is generally better than stainless steel for most reactive substances. Titanium alloys are attacked by hydrofluoric acid and acid containing fluorides, at room temperature, but resistant to almost all other corroding media. They also show excellent stress corrosion behavior except in red fuming nitric acid. Titanium alloys show excellent atmospheric and marine corrosion resistance. Cavitation resistance of Ti-6-4 alloy in water is superior to stainless steel. Due to excellent corrosion resistance shown by titanium and its alloys, they find extensive applications in heat exchangers, reactor vessels desalination plants, steam turbine blades, condenser tubings and several other components in chemical, marine, petrochemical, offshore and power generation industries. Its non-toxicity and biocompatibility in addition to excellent corrosion resistance, is made use of in prosthetic devices such as heart-valve parts and leg bone replacements or splints. Application related to corrosion resistance, and bio-compatible properties account for about 30% titanium.

Majority of demand for titanium alloys, however, is from aerospace industries where high specific strengths make them an attractive choice for airframes, blades and other parts of both low as well as high-pressure compressors of turbine engine. Though strength is

the prime consideration for such applications, other requirements like fatigue life, fracture toughness, creep resistance, microstructural stability at high temperatures may also have to be met depending on nature of application. To meet these multifarious requirements different alloys have been developed.

## 2.3 Classification of Titanium alloys [6]

Titanium alloys are classified according to phases present in their structure. Alloys that consist mainly of the  $\alpha$  phase are called  $\alpha$  alloys, whereas those that contain principally the  $\alpha$  phases along with small amounts of  $\beta$ -stabilizing elements are termed near-  $\alpha$  titanium alloys. Alloys that consist of mixtures of  $\alpha$  and  $\beta$  phase are classified as  $\alpha$  - $\beta$  alloys. Finally, titanium alloys in which  $\beta$  phase is stabilized at room temperature after cooling from a solution heat treatment are classified as  $\beta$  alloys. Each group has certain distinguishing characteristics, which are briefly described below.

As described earlier pure titanium has two allotropic forms, the low temperature hcp  $\alpha$  phase and the elevated temperature ( $\alpha \rightarrow \beta$ ) bcc  $\beta$  phase, the allotropic transformation temperature being 882.5 0C (1155.5 K) [7,8]. Alloying elements added tend to preferentially stabilize one or other of the three phases.

Elements like Al, C, O, N, Sn, etc., when added to titanium raise the transformation temperature (commonly referred to as  $\beta$ -transus) of the alloy and thus stabilize the  $\alpha$  phase to a temperature higher than 882.5  $^0$ C. These elements are referred as  $\alpha$  stabilizer. Rosenberg has suggested has suggested the following expression [9] for aluminum equivalent Al\* of the alloy:

$$\text{Al}^* = [\text{Al}] + [\text{Zr}]/6 + [\text{Sn}]/5 + 10 [\text{O}+\text{C}+2\text{N}] \text{ wt\%}$$

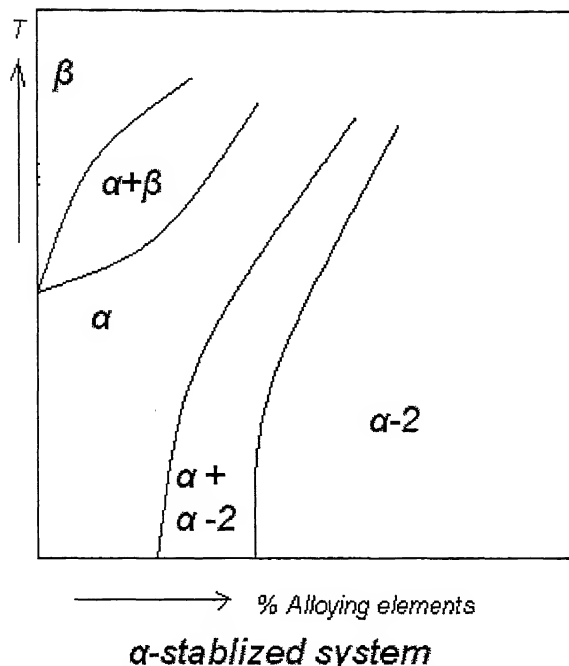
Elements like Mo, V, Mn, Cu, Cr, Fe, H, Si when added to titanium, lower the  $\beta$ -transus temperature and hence are known as  $\beta$  stabilizers. Molchanova [7] has suggested the following expression for Mo equivalent Mo\* of the alloy:

$$\begin{aligned} \text{Mo}^* = & [\text{Mo}] + [\text{Ta}]/5 + [\text{Nb}]/6 + [\text{W}]/1.5 + [\text{V}]/1.5 + 1.25 [\text{CR}] + 1.25 [\text{Ni}] + \\ & 1.7[\text{Mn}] + 1.7 [\text{Co}] + 2.5 [\text{Fe}] \end{aligned}$$

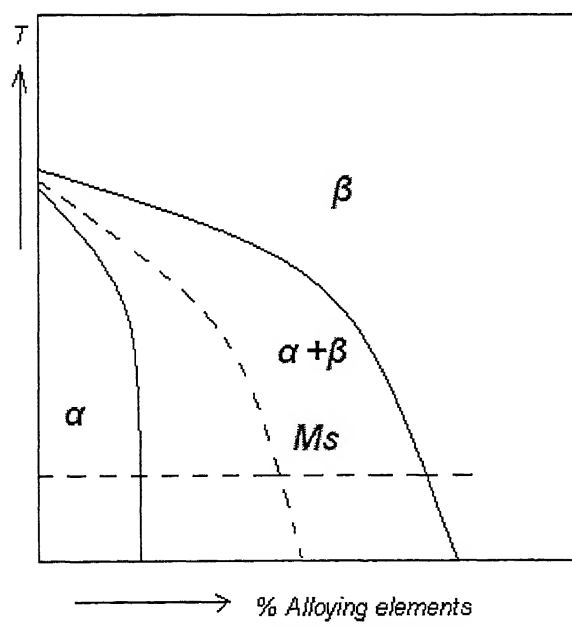
Titanium  $\alpha$  stabilizer and titanium  $\beta$  stabilizer phase diagrams [10] due to variation in alloying elements of different nature are shown in fig 2.2. Figure 2.2 (a) represents  $\alpha$ -stabilizing alloying addition; indicating increasing alloying addition result in increase in  $\beta$  transus temperature, to eventually formation of a hexagonal ordered compound  $\alpha_2$ .

The figure 2.2 (b) represents equilibrium diagram for  $\beta$  stabilizers, indicating increasing alloying addition result in both a decrease of  $\beta$  transus temperature and the volume fraction of the low temperature  $\alpha$ -phase present at particular temperature. Thus the type and concentration that forms the basis for classification of titanium alloys. Depending on the type alloying addition made, titanium alloys can be made  $\alpha$ , near  $\alpha$ ,  $\alpha + \beta$ , near  $\beta$  or  $\beta$  alloys.

Figure 2.2 represents that increasing  $\alpha$  stabilizing alloy addition results in increase in  $\beta$  transus temperature, to eventually the formation of a hexagonal ordered compound  $\alpha_2$ .



(a).



(b)

Fig 2.2 a-b      Schematic Diagrams of Binary Titanium Alloy System

### 2.3.1 $\alpha$ -Titanium Alloys

All  $\alpha$  **titanium** alloys have HCP crystal structure of titanium. These alloys contain only  $\alpha$  stabilizer as alloying elements. Due to single-phase nature of  $\alpha$  titanium alloys no microstructural strengthening can be achieved in these kind of alloys. Solid solution strengthening [9] of these alloys is also limited because an aluminum equivalent of more than 9.0 promotes the formation of brittle phase of  $\alpha_2$ . These alloys are characterized by satisfactory strength, good notch toughness, and good creep resistance and weldability [11]. These alloys are generally non-heat-treatable and weldable. Furthermore due to absence of ductile to brittle transformation, a property of the bcc structure renders  $\alpha$  alloy suitable for cryogenic applications [12]. However these alloys have poor workability.

Aluminum is the one of the important alloying elements for titanium since it strengthens the later by solid solution strengthening and also reduces its density. Tin is added to Ti-5% Al-2.5%Sn since it also contributes solid solution strengthening. Oxygen, which is present to a certain degree in all titanium alloys, is also a strong  $\alpha$  stabilizer like aluminum and strengthens titanium. However, like all interstitial elements in titanium, oxygen lowers its ductility [13]. Some of the important  $\alpha$  Alloy is shown in table 2.3 [11].

### 2.3.2 Near $\alpha$ -Titanium Alloys

Near  $\alpha$  -Titanium Alloys are those that contain some  $\beta$  phase dispersed in an otherwise all  $\alpha$  -phase structure. Small addition molybdenum and vanadium (about 1-2 percent), which are  $\beta$ -stabilizing elements, are added to these alloys to retain some  $\beta$  phase at room temperature. By such additions problems related to low strength and poor workability of high aluminum compositions are eliminated and a compromise is effected between the higher strength which is available with alpha -beta ( $\alpha +\beta$ ) alloys and better high temperature stability and weldability which are characteristics of  $\alpha$  alloys. Of the near- $\alpha$  titanium alloy, Ti-8%Al-1%Mo-1%V, and Ti-6% Al- 2% Sn-4% Zr-2% Mo alloys are most commonly used and account for about

3 percent of titanium market. These alloys are used in moderately high temperature applications in the compressor section of jet engines and have been used for aircraft skin components. Some of the important Near- $\alpha$  Titanium alloys are given in table 2.3. [23].

### 2.3.3 $\alpha + \beta$ Titanium alloys

This class of titanium alloys contains one or more  $\beta$ -stabilizing elements in sufficient quantity to permit the retention of appreciable amounts of beta phase at room temperature [6], resulting in  $\alpha + \beta$  structure.  $\alpha + \beta$  titanium alloys can be solution heat treated, quenched, and aged for increased strength. Morphology of both the phases ( $\alpha$  or  $\beta$ ) can be considerably varied by controlling various heat-treatment and mechanical working parameters. A wide range of different property levels can therefore be achieved in these alloys. This class of alloys generally exhibits good fabricability as well as high room temperature strength. They may contain between 10 to 50 %  $\beta$  phase at room temperature; if they contain more than 20% they are not weldable. The chemical composition of the most important of these alloys is listed in table 2.3.

Ti – 6% Al – 4% V is by far the most important and widely used titanium alloy, accounting more than 60 % titanium market. It can be readily welded, forged, and machined, and is available in a wide variety of mill product forms such as sheet, extrusions, wire, and rod. Ti - 6% Al -4% V is also used extensively for ordnance forgings. It is heat-treatable to an ultimate tensile strength of 1130 MPa and has good metallurgical stability to 482  $^{\circ}\text{C}$ . One of its disadvantages is that, since it is lean  $\alpha$ - $\beta$  alloy, it has low hardenability, so that sections of only up about 1 inch can be hardened all the way through. Applications of these alloys include components of advance jet engines and other structural components in aerospace industry.

### 2.3.4 Near- $\beta$ Titanium alloys

Still larger addition of  $\beta$ -stabilizers can cause retention of  $\beta$  phase at room temperature. These alloys are called near  $\beta$  alloys [6]. These alloys show excellent cold formability in which high strengths can also be achieved through proper heat treatment. Examples of some of these alloys are these alloys are shown in table2.3. This family of alloys has emerged for commercial applications only in recent past.

### 2.3.5 $\beta$ Titanium alloys

If sufficient amount of  $\beta$ -stabilizing elements are added to titanium, a structure consisting of all metastable  $\beta$  phase can be obtained at room temperature by quenching or even in some cases by air-cooling. The principal alloying elements for  $\beta$  titanium alloys are vanadium, molybdenum, chromium, and iron. Zirconium is sometimes added since it strengthens both the  $\beta$  and  $\alpha$  phase. Aluminum is also added to most of these alloys since it lowers their density, adds some solid-solution hardening, and improves oxidation resistance. The chemical composition and typical applications of the current  $\beta$  titanium alloys are given in table 2.3.

These alloys have high densities, poor ductilities, poor oxidation resistance and less commercial importance. These alloys according to Wood [11], are extremely formable. They are, however, prone to ductile to brittle transition [14] and along with other bcc phase alloys, are unsuitable for low temperature applications [12]. Some of the beta alloys are shown in table 2.3 [15,16]. Ti-Nb alloys can be used as low temperature superconductors but their commercial application is not very high.

Since our present investigation is concerned with Ti-10V-4.5 Fe- 2 Al (wt%), a  $\beta$ -Titanium alloy, and Ti-22 (at%)Al- 25 Nb- 0.5 Mo, an intermetallic (O+B2) the discussion henceforth will only be confined to the  $\beta$  titanium alloy and Titanium Aluminide (O+B2) alloys only.

## 2.4 Microstructural Features of titanium alloys [17,18,19]

Microstructures are characterized by the nature of phases present, their shape, size, and morphology that, in turn, are functions of heat treatment and working schedule. Some common microstructural features are listed below.

**Table 2.3 Classifications of U.S. Technical Multicomponent Alloys**

Composition (wt%)	Classification
Ti-5 Al-2.5 Sn	$\alpha$
Ti-8 Al-1Mo-1 V	
Ti-6 Al-2 Sn-4 Zr- 2Mo	Near $\alpha$
Ti-6 Al-4 V	
Ti-8 Al-6 V-2 Sn	$\alpha + \beta$
Ti-3 Al-2.5 V	
Ti-6 Al-2 Sn-4 Zr- 6Mo	
Ti-6 Al-2 Sn-2 Zr- 4Cr-4Mo	Near $\beta$
Ti-10 V-2 Fe -3 Al	
Ti-13 V- 11 Cr- 3Al	
Ti-15 V- 3 Cr- 3Al-3 Sn	$\beta$
Ti-3 Al-8 V-6 Cr-4 Mo-4 Zr	
Ti-8 Mo-8 V-2 Fe-3 Al	
Ti-11.5 Mo-6 Zr- 4.5 Sn	

- a) **Primary  $\alpha$  ( $\alpha_p$ )** - It refers to the  $\alpha$  phase in a crystalline structure that is retained from the last high temperature ( $\alpha + \beta$ ) working or heat treatment. Morphology of primary  $\alpha$  is influenced by prior thermomechanical history and may vary from lamellar to equiaxed or mixed grains.
- b) **Alpha Prime ( $\alpha'$ )** - A supersaturated non-equilibrium hexagonal  $\alpha$  phase formed by a diffusionless transformation of the beta phase. It occurs as fine, randomly oriented needles
- c) **Secondary  $\alpha$  or transformed  $\beta$**  - A local or continuous structure, comprised of decomposition products arising by nucleation and growth during cooling through the sub-transus region. Primary and regrowth  $\alpha$  may be present, it typically consists of  $\alpha$  platelets that may or may not be separated by  $\beta$  phase.
- d) **Grain Boundary  $\alpha$**  - Primary alpha outlining prior beta grain boundaries are referred as grain boundary alpha. It evolves by heterogeneous transformation when cooled slowly

from the  $\beta$  to  $\alpha+\beta$  phase field. Thickness and continuity of the layer depends on cooling rate and alloy composition.

- e) **Alpha Double Prime ( $\alpha''$ )** - It refers to a supersaturated, non-equilibrium orthorhombic phase formed by diffusionless transformation of the beta phase in certain alloys like Ti-Mo, Ti-Nb etc. which have high concentration of beta stabilizers.
- f) **Metastable  $\beta$**  - Refers to beta phase, which is retained at room temperature instead of undergoing martensitic transformation. Prior beta grain boundaries are visible whose sizes are function of temperature and time of solutionizing in the beta phase field.
- g) **Alpha-2 ( $\alpha_2$ )** - It refers to ordered alpha phase  $Ti_3Al$  produced by segregation of alloying elements and existing as small precipitates.
- h) **Silicides** - In high silicon bearing alloys silicon combines with titanium and other alloying elements to form complex compounds known as silicides e.g.,  $Ti_5Si_3$ , Ti-Mo-Si et. Which exist as precipitates in the matrix.
- i) **Omega phase( $\omega$ )**- A non equilibrium, submicroscopic phase formed either isothermally during aging at about  $475^0C$  or athermally during quenching, often thought to be a transition phase during the formation of  $\alpha$  from  $\beta$ .
- j) **Gamma phase ( $\gamma$ )**- An ordered structure of Ti-Al compound.
- k) **Hydride Phase ( $TiH_x$ )**- The phase  $TiH_x$  forms in Titanium when the Hydrogen content exceeds the solubility limit.
- l) **Interface phase**- It is a reaction product that forms at the interface between  $\alpha$  and  $\beta$  phases of alloys like Ti-6Al-4V, probably due to hydrogen absorption. It has both bcc and hcp forms.

**Table 2.4 Typical room temperature Tensile Strengths of some commercial Titanium based alloys**

Alloy name	Nominal composition	Condition	UTS $10^8 \text{Nm}^{-2}$	YS $10^8 \text{Nm}^{-2}$	% Elong.
5-2.5	Ti-5Al-2.5Sn	A, 25-4h, 705-870°C	8.3-9.0	7.9-8.3	13-18
3-2.5	Ti-3Al-2.5Sn	A, 1-3,650-760°C	6.5	6.2	22
6-2-1-1	Ti-6Al-2Nb-1Ta-1Mo	A, 25-2h, 705-925°C	8.6	7.6	14
8-1-1	Ti-8Al-1Mo-1V	A, 8h, 790°C	10.0	9.3	12
Corona 5	Ti-4.5Al-5Mo-1.5Cr	$\alpha$ - $\beta$ A, after $\beta$ processing	9.7-11.0	9.3-10.3	12-15
Ti-17	Ti-5Al-2Sn-2Zr-4Mo-4Cr	$\alpha$ - $\beta$ or $\beta$ processed Aged	1.4	10.7	8
6-4	Ti-6Al-4V	A, 2h, 705-875°C Aged	9.6 11.7	9.0 11.0	17 12
6-6-2	Ti-6Al-6V-2Sn	A, 3h, 705-845°C Aged	10.7 12.8	10.0 12.1	14 10
6-2-4-2	Ti-6Al-2Sn-4Zr-2Mo	A, 4h, 705-845°C	10.0	9.3	15
6-2-4-6	Ti-6Al-2Sn-4Zr-6Mo	A, 2h, 815-870°C Aged	10.3 12.1	9.7 11.4	11 8
6-22-22	Ti-6Al-2Sn-2Zr-2Mo-2Cr-0.25Si	$\alpha$ - $\beta$ processed + Aged	10.0	10.1	14
10-2-3	Ti-10Al-2Fe-3V	A, 1h, 760°C Aged	9.7 12.4-13.4	9.0 11.4-12.4	9 7
15-3-3-3	Ti-15V-3Cr-3Sn-3Al	A, 0.25h, 790°C Aged	7.9 11.4	7.7 10.7	20-25 8
13-11-3	Ti-13V-11Cr-3Al	A, 0.5h, 760-815°C Aged	9.3-9.7 12.1	8.6 11.4	18 7
38-6-44	Ti-3Al-8V-6Cr-4Mo-4Zr	A, 0.5h, 815-925°C Aged	8.3-9.0 12.4	7.8-8.3 11.7	10-15 7
$\beta$ -3	Ti-4.5Sn-6Zr-11.5Mo	A, 0.5h, 705-870°C Aged	6.9-7.6 12.4	6.5 11.7	23 7

A→Annealed

**Table 2.5 Comparative properties of some metals**

Metal	UTS (10 <sup>3</sup> psi)	Y.S. (10 <sup>3</sup> psi)	Elong. %	R.A. %	Mod.of Elasticity (10 <sup>6</sup> psi)	Mod.of Rigidity (10 <sup>6</sup> psi)	BHN*	Charpy Impact (ft-lb)
Al	9	3	60	70	10	3.87	15	19
Cu	37	14	15	52	16	6	47	16
Mg	40	20	40	80	29.7	10	90	-
Fe(pure)	27	10	15	50	6.25	2.4	37	-
Fe(ingt)	44.3	22.7	47	75	29.1	11.6	120	19
Ti(pure)	35	20	55	80	15	5	85	100
Ti(ingt)	75	55	25	50	16	5	180	30

\* Ferrous and titanium metals measured with 3000-kg load and a 10-mm ball, other metal measured with a 500-kg load and a 10-mm ball.

**Table 2.6 Comparative properties of some alloys**

Alloy	UTS ( $10^3$ psi)	Y.S. ( $10^3$ psi)	Elong. %	R.A. %	Mod.of Elast. ( $10^6$ psi)	Mod.of Rigidity ( $10^6$ psi)	BHN *	Charpy Impact (ft-lb)
Ti (3Al- 5Cr)	150	135	18	45	17	6	290	24
Steel (4340)	145	135	20	58	28.7	12	285	52
Stainless Steel (18-8)	89.4	28	61	75	29	-	140	-
Al (4S-O)	26	10	25	50	10	3.9	45	-
Al (75S- T6)	82	72	11	40	10.4	3.9	150	-
Mg (AZ31)	37	22	21	25	6.5	2.4	56	3.2

\* Ferrous and titanium metals measured with 3000-kg load and a 10-mm ball, other metal measured with a 500-kg load and a 10-mm ball.

## 2.5 LAMINATE METAL COMPOSITES [21]

Laminated metal composites consist of alternating metal or metal containing layers that are bonded with sharp interfaces. These are important engineering materials by virtue of their attractive combination of strength and fracture resistance. Damage critical properties (such as fracture toughness, fatigue and impact behavior) can be superior to those exhibited by component materials. The damage critical properties are strongly influenced by local delaminations at the layer interfaces.

Earliest known reference to improved properties in a laminated metal composite according to archeological records show that solid state joining of two dissimilar ferrous materials was being practiced as early as first millennium BC. A photomicrograph taken of an adze blade (a cutting toll used in farming), made by Greek blacksmiths around 400 BC, shows a fairly sharp interface between the medium carbon steel cutting blade adjoining the low carbon backing plate. In more recent times, beginning in the period around AD 500, pattern welded daggers and swords were made. Included in this group of materials are the Norwegian (Viking) blades, the Chinese welded swords, the Indonesian kris, and Japanese swords. These weapons were probably made more for their aesthetic appearance than for their destructive qualities (figure2.3).

### 2.5.1 Formation of laminates

Formation of laminate metal composites can be categorized into three groups, bonding, deposition and spray forming. In bonding techniques material in sheet or plate form solid state bonded at the interfaces. In the case of deposition techniques, layers of component materials are formed sequentially by atomic or molecular scale transport of the component materials. Spray forming techniques, on the other hand, involve direct deposition of molten metals of the component materials into laminate form.

### 2.5.2 Bonded laminates

Bonding techniques may be classified into a number of subgroups, such as, adhesive bonding, melt bonding, diffusion bonding, reaction bonding, deformation bonding etc. surface preparation of the component materials, bonding temperature and pressure,

interdiffusion, and chemical reactions between the component materials greatly influence the microstructure, chemistry, and bond strength at the interfaces, and overall physical and mechanical properties of the resulting laminates.

- a) **Adhesive Bonding:** Here adhesion is done by epoxy adhesives, which results in extremely high interfacial bond strength. The bonds could be made so strong that the laminates do not delaminate when pulled to fracture. Early version of aluminum laminates was bonded by these methods.
- b) **Melt bonding:** Here adhesion is done by dipping the one layer of the laminate in the melt of the other layer of the laminate. e.g. multilayer laminates of plain carbon steel and zinc by dipping the steel sheets in molten zinc. The molten zinc between the sheets acted as glue and solidified to form zinc / steel laminates.
- c) **Infiltration:** Here layers of the two materials were sandwiched and then heated to above the melting temperature of one of the layer and subsequent infiltration, e.g. layers of Al sandwiched in between boron carbide tapes.
- d) **Diffusion bonding:** In diffusion bonding, the component materials were stacked together in vacuum hot press and heated to near the solutionizing temperature. A low pressure (compared to large scale plastic flow) was applied to facilitate diffusion bonding.
- e) **Reaction bonding:** Here two materials are stacked and then heated, the two stacking material may form an intermetallic due to reaction between the two, e.g. Al and Ni foils when stacked together and heated at  $600^{\circ}\text{C}$  results in the formation of intermetallic NiAl at the Al and Ni interfaces. By adjusting the relative thickness of the foils, multilayer laminates of Al/ NiAl or Ni/ NiAl could be created.
- f) **Deformation bonding:** Here layers of the component materials are stacked and subjected to large plastic deformation until they are bonded together. It is one of the most efficient techniques from the industrial processing viewpoint, and includes press, roll, and co-extrusion. The first two techniques are used for making LMCs in plate and sheet form, and fourth technique is used for producing laminates of rod shape.

### 2.5.3 Deformation response of laminate during deformation bonding

In deformation bonding components are subjected to large plastic strains during processing. The plastic flow helps promote a strong bond between component of the laminate

by placing the individual components of the laminate into close contact and breaking oxide films and impurity layers that may interfere with the bonding process. The deformation behavior of a laminate during processing can be understood from the strain rate stress behavior of the individual components (fig 2.4). In the plot in fig 2.4 shows a system in which the component materials have distinctly different strain rate-stress behavior. The shaded area within the curves for the individual components defines the strain rate-stress response for the laminate. The upper bound for the flow stress of the laminate at a given strain rate is defined by isostrain behavior, in which each component of the laminate undergoes the same strain. In practice, isostrain behavior is approached when individual component layers are thin and frictional constraints or bonding between layers enforces uniform deformation. The lower bound for the flow stress of the laminate at a given strain rate is defined by isostress behavior, in which each component is subjected to same stress. Isostress behavior requires the individual layers to act independently, and thus this kind of behavior is approached for thick layer systems. The ideal strain rate and temperature for processing are chosen so that the components of the laminate have comparable flow stresses, which limit the extent to which one component can preferentially extrude from the laminate during processing. In thin layer system flow stress and temperature range could be high because frictional forces tend to enforce uniform deformation and tendency to isostrain behavior.

## 2.5.4 Tensile behavior of Laminate Composites

### a) Tensile properties of ultrafine layer, laminated metal composites

These composites are usually prepared as foil samples, and typically only their breaking strength is documented. Figure 2.5 shows the tensile strength of such materials processed by electrodeposition or by sputtering. The data are for copper, layered with nickel or Monel. The figure shows the breaking strength (equivalent to UTS) as a function of the reciprocal square root of the multilayer periodicity width (also called as modulation width). For each set of data, a Hall-Petch type relation is observed, i.e. a linear relation is observed over a range of laminate layer spacing, the strength increasing with the decrease in modulation width. This trend suggests that barrier spacing is a crucial factor in controlling

the strength of the laminate. From the figure, it is clear that there is an optimum width and the strength decreases with further decreases in modulation width.

### **b) Tensile properties of thick layer laminated composites**

These kind of laminated composites are usually prepared by solid state bonding procedures. The bonding step commonly involves mechanical working by pressing, forging, rolling, and extrusion. The tensile yield strength of thick layer laminated metal composites can readily predict by the rule of averages. This has been shown for metal systems where two components of equal volume fractions have been investigated. For these cases, the relation describes the rule of averages

$$\sigma_y = 0.5 (\sigma_y)_A + 0.5 (\sigma_y)_B$$

Where  $\sigma_y$  is the tensile strength of the composite,  $(\sigma_y)_A$  is the yield strength of the strong component and  $(\sigma_y)_B$  is the yield strength of the weak component. Figure 2.6 shows the application of the above equation for predicting the normalized strength of the laminate (normalized by the stronger component) as a function of the yield strength ratio of the of the component materials.

### **c) Tensile Ductility of Laminate Composites**

Tensile ductility of the laminated composites can not be predicted by the rule of averages. This is because the tensile ductility of laminates is dependent on many variables, including the susceptibility of the less ductile layer to cracking, the contribution to cracking from the interlayer region, the ease of delamination, and most importantly the influence of layer thickness (fig 2.7).

From the figure 2.7 it is clear that tensile ductility of most of the laminated composites is lower than that predicted from the rule of averages when the difference between ductility of the two components is large. This low ductility can be related to the susceptibility of the less ductile layer to early cracking.

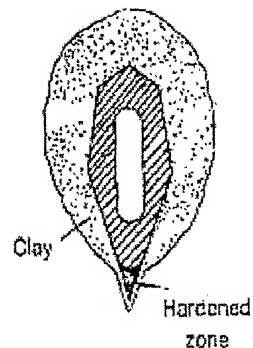
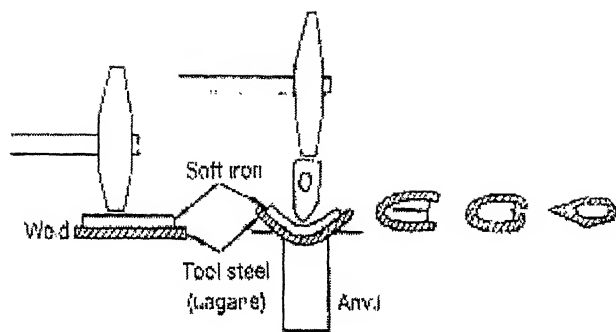
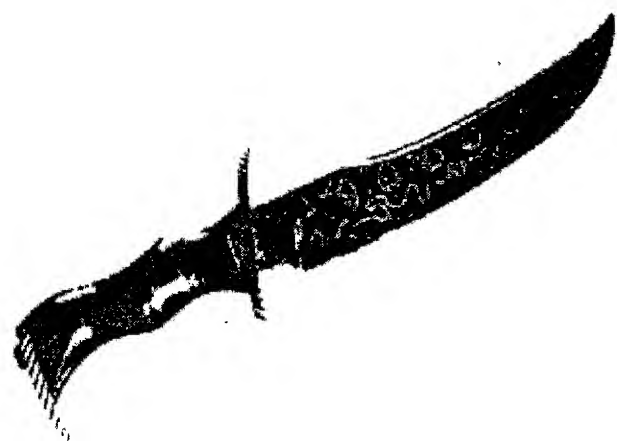
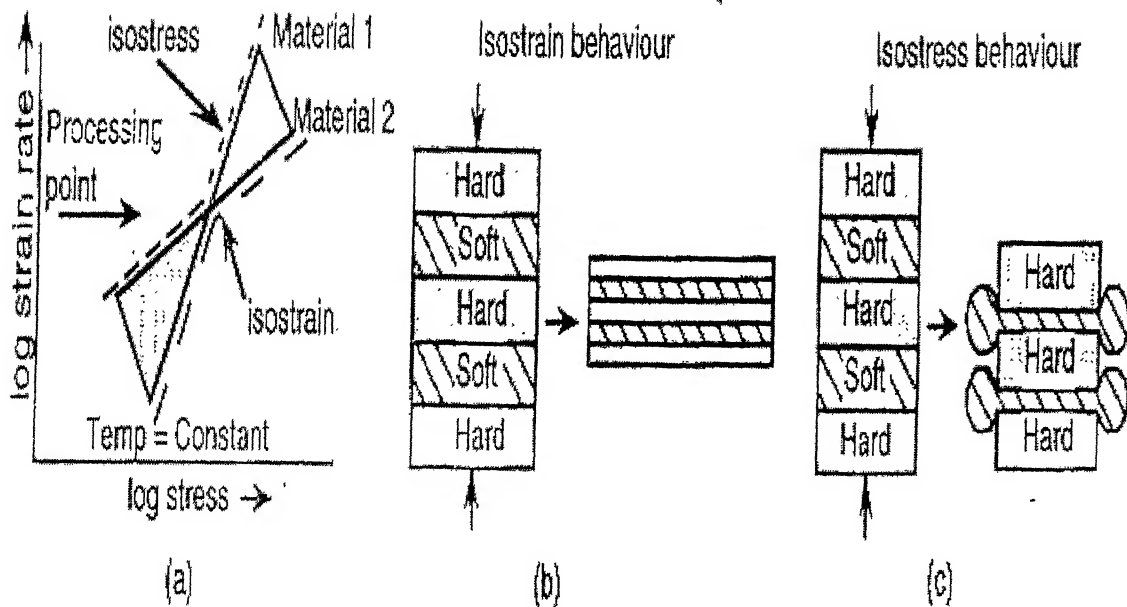
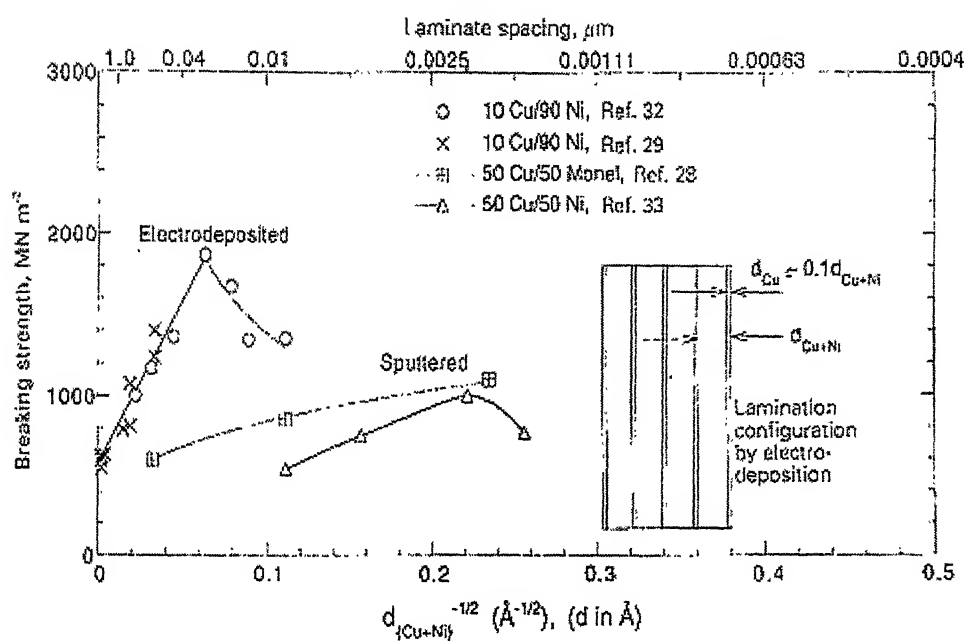


Fig 2.3 (a) Welded Damascus steel knife made by American blacksmith (b) Procedure used by Japanese blacksmiths to make laminated tools by solid state bonding ultrahigh carbon steels, known as uagane, to soft iron



**Fig 2.4 Deformation response of the laminate during press bonding**

(a) strain rate stress response (b) isostrain behavior (c) isostress behavior



**Fig 2.5** Breaking strength of ultrathin layer laminated composites as a function of modulating spacing  $d$  (as  $d^{-1/2}$ ): laminates are based on layers of Cu alternating with either Ni or Monel layers

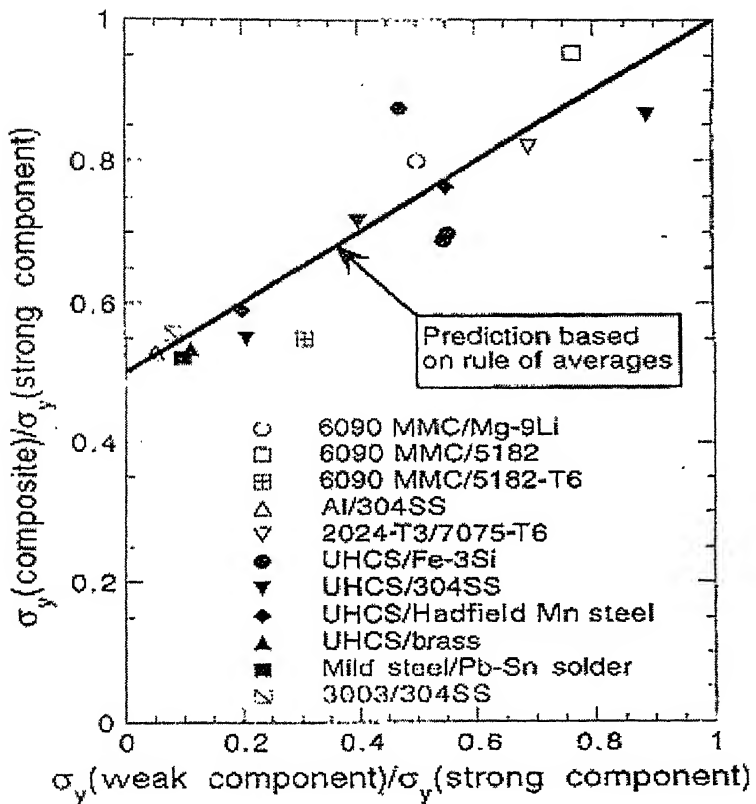


Fig 2.6 Experimental yield strength of a thick layer laminated composite

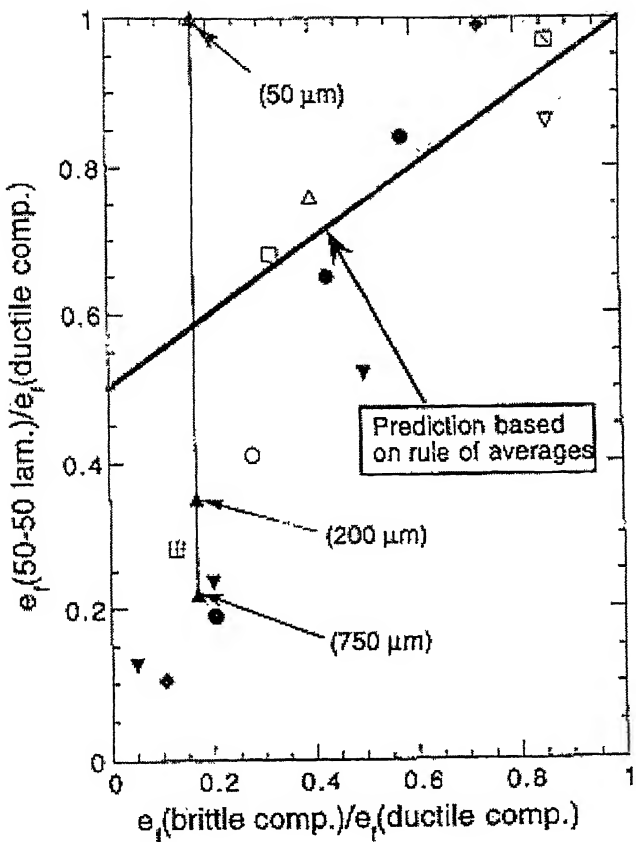


Fig 2.7 Experimental tensile elongation to fracture curve

# Chapter 3

## EXPERIMENTAL PROCEDURE

### 3.1 Material for the present investigation

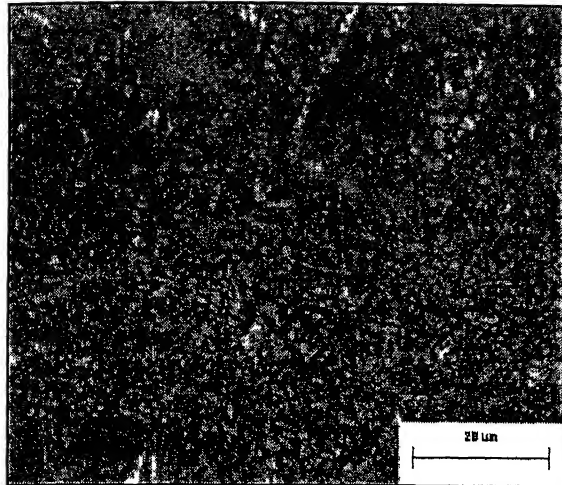
Starting material for the study consists of laminated composite having alternate layers of  $\beta$ -Titanium alloy and Titanium Aluminide (O+B2) prepared by vacuum arc melting in the form of pancakes. The chemical composition of these alloys is given below in the table 3.1. These pancakes were hot rolled, ground and pickled and then finally cold rolled to 1 mm thickness sheets.

From these sheets laminate composite material is prepared by sandwiching twelve alternate layers consisting of  $\beta$  Titanium alloy and Titanium Aluminide. Cold rolled sheets of the two alloys were stacked together and hot pressed at about  $800^{\circ}\text{C}$  and 130 MPa pressure.

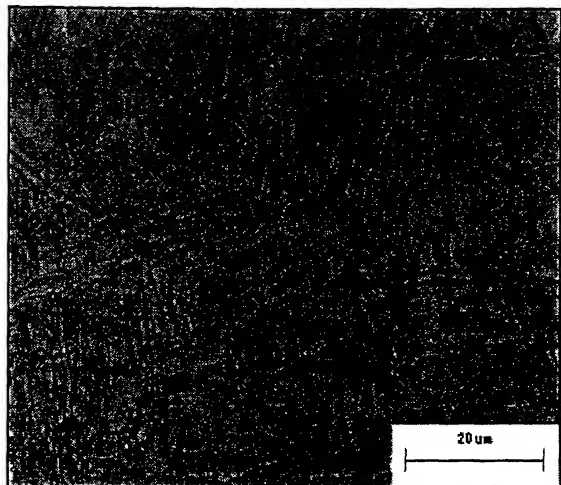
The processed laminate composite shows a defect free structure across the  $\beta$  Titanium Alloy /Titanium Aluminide interface. Microstructures of the as pressed composite are shown in the figure 3.1a-b. The dimensions of the starting material is given in fig 3.1c

**Table 3.1. Chemical composition of the material used in the investigation**

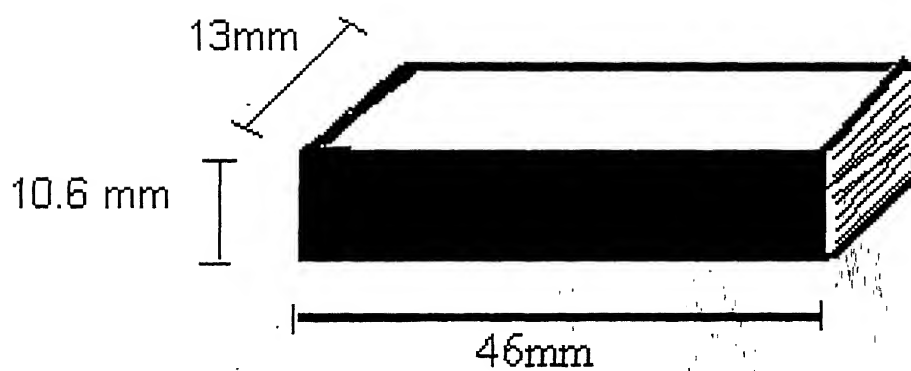
Material	Al wt%	Nb/V wt%	Mo/Fe wt%	O in ppm	N in ppm
$\beta$ Ti-alloy	1.71	9.5	4.1	700	80
Ti – Aluminide	10.4	43.5	1.3	600	180



(a)



(b)



(c)

**Fig 3.1** (a) Microstructure of Aluminide phase of the as received sample at 500X.  
(b) Microstructure of  $\beta$  alloy phase of the as received sample at 500X.  
(c) Shape and Dimensions of as received sample

## 3.2 Thermo-mechanical treatment

### 3.2.1 Hot Rolling

Hot rolling process was carried out on a laboratory 2-high rolling mill with 135 mm diameter rolls and rolling speed of 55 rpm. In the present work, samples (10.6x 13x 46 mm) were heated at different temperatures for 30 minutes in a specially designed calibrated high temperature furnace having argon gas inlet, kept very close to the rolling mill to avoid much heat loss. The first sample was hot rolled at 1050 °C to 7.4 mm thick sheet initially (30% reduction) with four passes, subsequently it has been reduced to 1.8mm thick sheet in eight number of passes. The other two samples were hot rolled at 1000 °C and 950 °C respectively to 2.3 mm thick sheet and 2 mm thick sheet in ten and twelve number of passes respectively. No prior heating of the rolls were done before hot rolling of the specimens and they were maintained at room temperature. The inert argon atmosphere was maintained inside the furnace to prevent oxidation of the samples while heating and soaking.

The flow chart of thermo-mechanical treatment given is as shown in Figs. 3.2 All the hot rolling treatment involved soaking for 30 minutes initially and then 5 minutes after each pass and the rolling temperatures were of (a) 950°C (b) 1000°C and (c) 1050°C.

### 3.2.2 Warm Rolling

Sample hot rolled at 1000°C to 2.3 mm thickness was soaked for 10 minutes to homogenize it and then it is warm rolled at the temperature of 700°C to 1.4 mm sheet (~ 39% reduction) in eight number of passes. Utmost care was taken to avoid cracking of the sample.

# THERMOMECHANICAL TREATMENT OF THE MATERIAL

## Process flow chart

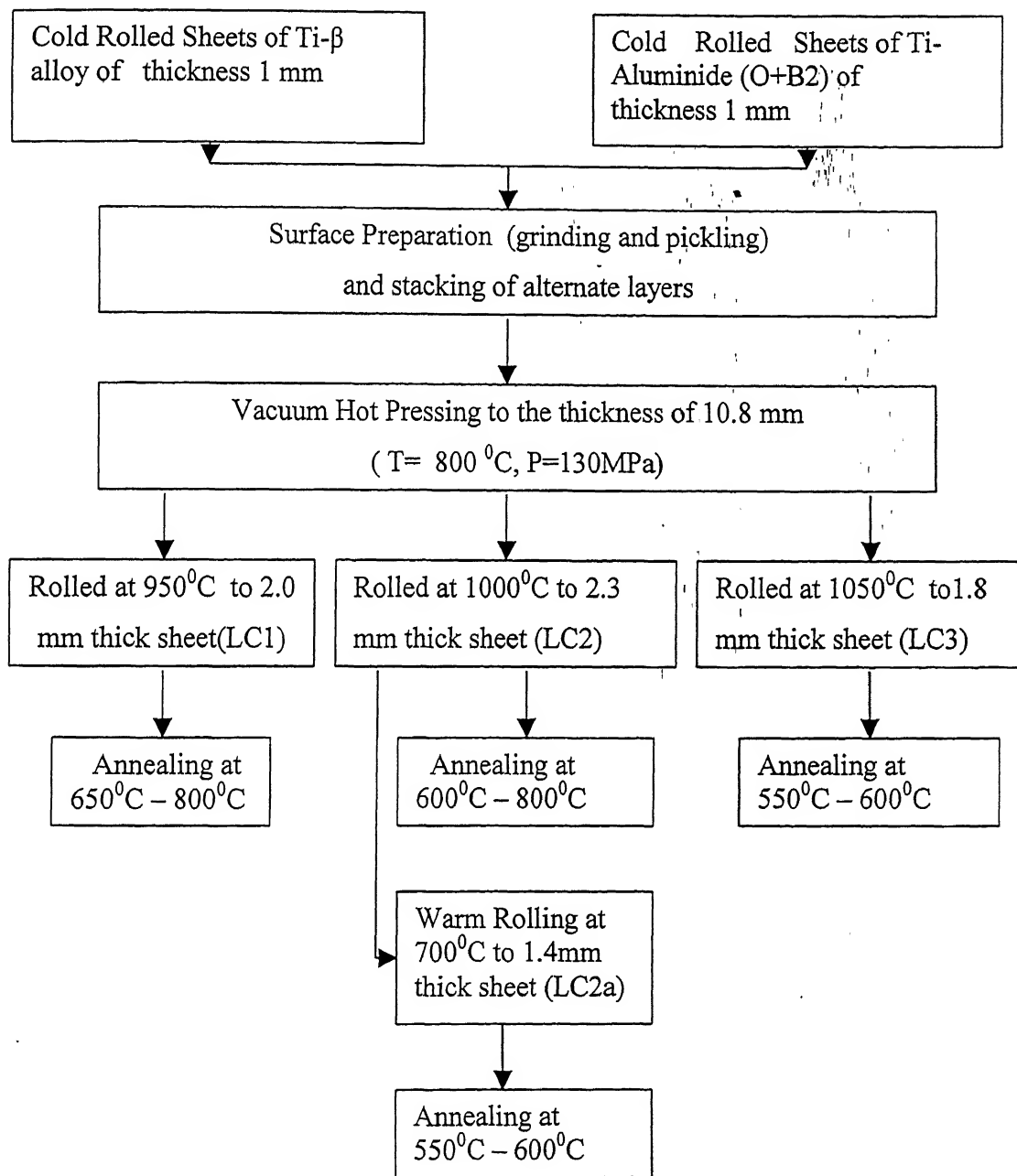


Fig 3.2 Process flow diagram

### 3.3 Microstructural characterization

#### 3.3.1 Sample preparation and optical microscopy

The microstructure samples were cut from the hot and warm rolled samples with diamond cutter. The samples were cut parallel to rolling direction and containing cross-section of alternate layers. These samples were given different heat treatments at the temperature range of  $550^{\circ}\text{C}$  to  $800^{\circ}\text{C}$  for different times. The heat-treated samples were mounted using hot mounting machine. The mounted samples were ground using a belt grinder followed by polishing on emery paper of various grades (1 to 4 grades) and wheel polishing with alumina powders of size  $1\text{ }\mu\text{m}$ ,  $0.3\text{ }\mu\text{m}$ ,  $0.05\text{ }\mu\text{m}$ . The mirrors like polished samples were etched using two different freshly prepared echants [38] alternatively for the  $\beta$  alloy layer and Aluminide layers.

1. Etchant 1: For  $\beta$ -Titanium alloy layer, the etchant used is Kroll's reagent having composition  $5\%$  HF +  $3\%$   $\text{HNO}_3$ + $92\%$   $\text{H}_2\text{O}$  for 20 to 30 sec.
2. Etchant 2: For Titanium Aluminide layer, the etchant used is Kroll's reagent having more HF content with composition  $8\%$  HF +  $3\%$   $\text{HNO}_3$ + $89\%$   $\text{H}_2\text{O}$  for 10 to 40 sec.

Leize wetzler optical microscope was used for low magnification microstructural study. The prepared samples were observed under the magnification of 100X; 200X and 500X using image analyzer.

#### 3.3.2 Quantitative microscopy

Aiolab Zeiss optical microscope with a maximum magnification 500X, connected to a computer by video input device, was used to acquire microstructural images. Image-pro plus imaging software tool was used for quantitative measurements. The captured images were subjected to quantitative measurements such as grain size and aspect ratio etc.

### 3.4 Mechanical Testing of the samples

#### 3.4.1 Microhardness Testing of the Samples

Microhardness of the samples at different thermomechanical and annealing treatment conditions were measured using the Leitz Miniload Microhardness tester under the load of 100gm. In each layer two indentations were made and average value of both the readings were taken for diagonal. After calculating average value en each layer again average value is taken for all the layers of  $\beta$ - phase and Aluminide phase.

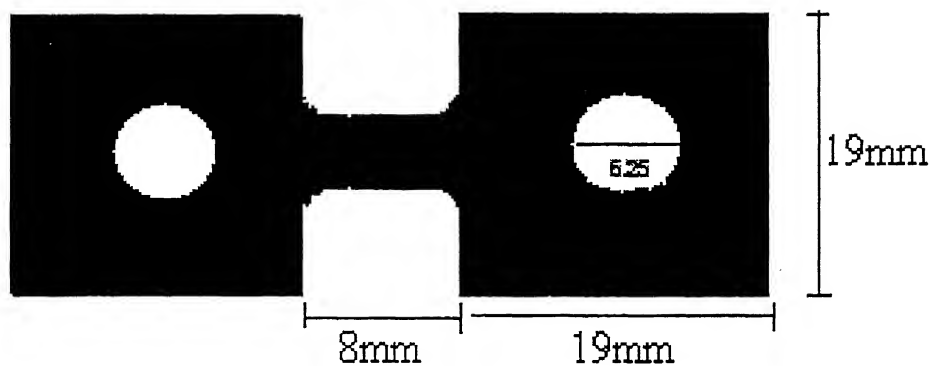
#### 3.4.2 Tensile Testing of the Samples

Tensile specimens were prepared according to ASTM standard as shown in Fig. 3.3. The specimens were prepared carefully to avoid the notch effect and pickled and cleaned properly. The high temperature testing of the processed sheets was done on the MTS machine model: 810.12. The furnace, attached to the machine, had a heating rate of  $200^{\circ}\text{C}/\text{Hr}$ . The samples were homogenized for 15 minutes at the desired temperature before start deforming. The initial strain rate taken for the tensile testing at higher temperatures was  $8*10^{-5}/\text{sec}$ .

The room temperature tensile tests were done at a crosshead speed of 0.5 mm/min (equivalent strain rate of  $1.4*10^{-4}/\text{sec}$  for the sample of gauge length 6 mm) in strain control mode using a closed loop servo-hydraulic material testing machine. The ultimate strength (UTS) and yield strength (YS) were calculated from the stress-strain curves. The toughness ( $U_T$ ) was approximated by the following expression [20].

$$U_T \approx \{(S_0 + S_u)/2\}e_f$$

where  $S_0$  is 0.2% offset yield strength,  $S_u$  is ultimate tensile strength and  $e_f$  is engineering strain at fracture



Gauge Length = 6mm  
Gauge Width = 5mm  
Gauge Thickness = 2mm  
Radius at the Corner = 1mm  
Hole Diameter = 6.25mm  
Total Length = 46mm

**Fig 3.3 Dimensions of Tensile Testing Specimen**

## Chapter 4

# RESULTS AND DISCUSSION

### 4.1 Rolling Behavior of Laminate Composite

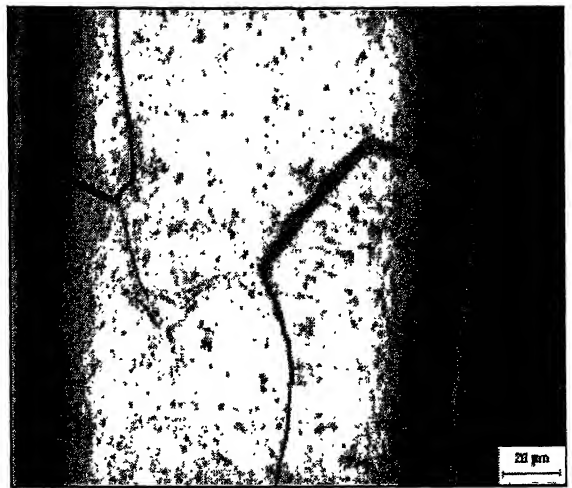
#### 4.1.1 Hot Rolling Behavior of Laminate Composite

The optical metallographic examination of the cross section of the as-received hot pressed  $\beta$ -titanium alloy-titanium aluminide laminate composite material showed a good defect free structure between the two interfaces namely the intermetallic aluminide phase and beta titanium alloy respectively. This absence of delamination at interfaces indicates good bonding characteristics of the two materials. Further microstructural examination of the hot pressed material showed that layers of both the phases in the composite had a non-uniform thickness along longitudinal direction. This waviness of the layers may be due to differential flow characteristics of the two constituent layers during the course of hot pressing.

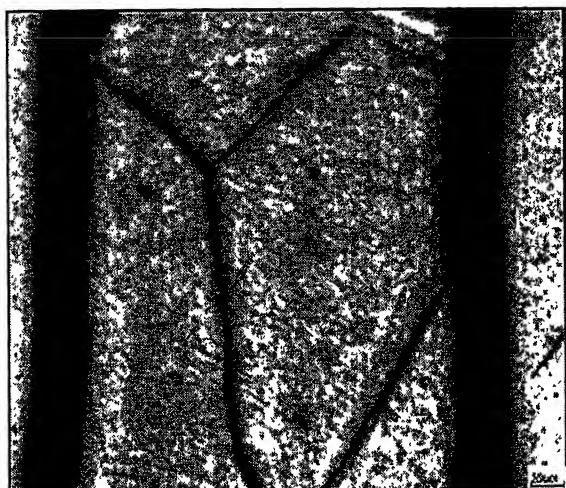
While up to about 15% thickness reduction in a single pass during hot rolling of the laminate composites at higher temperature i.e.  $1000^{\circ}\text{C}$  and  $1050^{\circ}\text{C}$  gave almost defect free microstructure without any delamination at the interfaces bonding, samples rolled at lower temperature, i.e. at  $950^{\circ}\text{C}$ , gave rise to cracking of edges which became more severe with increasing thickness reduction in a single pass. This observation indicates that the laminate composite had a reasonably good hot workability at temperatures higher than  $1000^{\circ}\text{C}$ . Because of these reasons the composites were given a total thickness reduction of 80 % to 85 % in 5 to 10 passes. It is worth mentioning that the  $\beta$  titanium alloy used for making the present laminate composites has the chemical composition of Ti-10V-4.5Fe-1.5Al and the  $\beta$ -transus temperature of about  $760^{\circ}\text{C}$ . All the hot rolling temperatures used in the present study were therefore above the  $\beta$  transus temperature of the metallic phase. Microstructure of  $\beta$  alloy region in laminates hot rolled at  $950^{\circ}\text{C}$ ,  $1000^{\circ}\text{C}$  and  $1050^{\circ}\text{C}$  are shown in Figure 4.1(a) – (d). It is seen that the  $\beta$  grains remain elongated in samples rolled at all the temperatures. Further, as the hot rolling temperature increased, the grains became coarser due to the rapid grain growth.



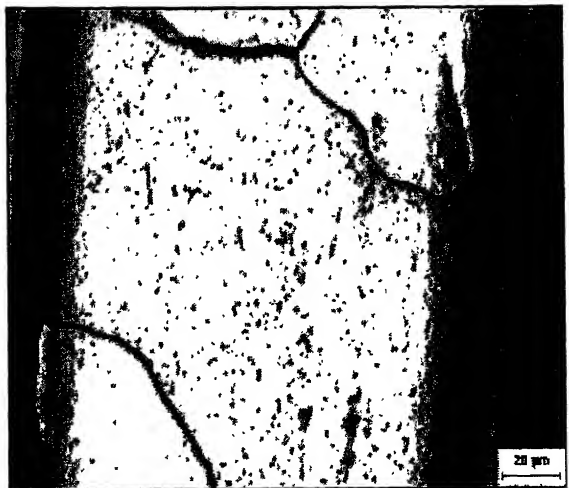
(a)  
(Mag 100X)



(b)  
(Mag 200X)



(c)  
(Mag. 200X)



(d)  
(Mag 100X)

**Figure 4.1** (a) Microstructures of the samples hot rolled at  $950^{\circ}\text{C}$ .  
(b) Microstructures of the samples hot rolled at  $1000^{\circ}\text{C}$ .  
(c) Microstructures of the samples hot rolled at  $1050^{\circ}\text{C}$  for 30% deformation.  
(d) Microstructures of the samples hot rolled at  $1050^{\circ}\text{C}$  for 83% deformation.

The presence of pancaked  $\beta$  grains in the metallic phase indicates that the material does not undergo dynamic recrystallization but deforms with only dynamic recovery taking place in it. Quantitative analysis of thickness after rolling indicated non-uniform reduction in thicknesses of the layers along longitudinal direction. This shows that there was no relative slip motion among the laminate layers and interface bonding between the two adjacent layers remained strong.

In contrast, the hot rolling temperature for the laminate composite was low for the deformation of the aluminide phase as its transus temperature is in the range of  $1050^0\text{C}$  -  $1060^0\text{C}$ . The as-deformed structure of the aluminide phase, however, could not be carefully examined due to its very poor response to etching by most of the conventional etchants tried. However, as shown in Figure-4.2(a) – (b), the structure of the aluminide phase was found to be much finer than that of the metallic phase. This also indicates that the hot rolling temperature remained below the transus temperature of the aluminide phase.

#### 4.1.2 Warm Rolling Behavior of Laminate composite

A few samples, hot rolled at  $1000^0\text{C}$ , were further warm rolled at  $700^0\text{C}$ , i.e. at a temperature below  $\beta$ -transus temperature of the metallic phase to about 39% thickness reduction in 8 passes. Observations during warm rolling suggest that cracking started even at relatively low deformation of 4% to 5% reduction in a single pass. Utmost care was, therefore, required to prevent cracking in the laminate composite. Microstructure of the laminate first hot rolled at  $1000^0\text{C}$  and subsequently warm-rolled to the thickness reduction of 39% at  $700^0\text{C}$  is shown in Figure 4.3. Since the warm rolling temperature is below the  $\beta$ -transus temperature, the microstructure of the metallic phase comprises of fine equiaxed  $\alpha$  grains in the matrix of  $\beta$ . Since the temperature of rolling is low, it is expected that  $\beta$  grains will remain in unrecrystallized form and would have a higher density of dislocations forming denser sub-grain boundaries. These equiaxed  $\alpha$  grains are expected to precipitate on these sub-grain boundaries.

## 4.2 Annealing Behaviour of Rolled Laminate Composite

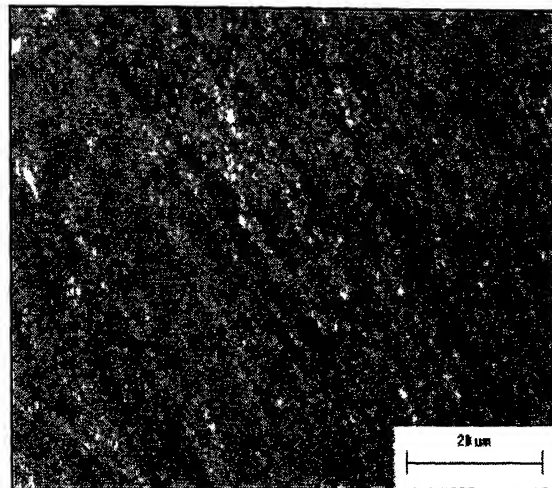
As mentioned in Section 4.1, microstructures of the laminate composite hot rolled at  $950^0\text{C}$ ,  $1000^0\text{C}$  and  $1050^0\text{C}$  comprised of coarse beta grains in the metallic layers and fine grains of alpha-2 in the aluminide layers. Further, as mentioned earlier  $\beta$  grains had elongated pancaked shape and were not recrystallized. Annealing operation was therefore performed on hot rolled laminate composites for obtaining the recrystallized structure in the metallic phase. This section gives the results pertaining to the annealing behaviour of rolled laminate composites.

### 4.2.1 Annealing of Composite Material Rolled at $950^0\text{C}$

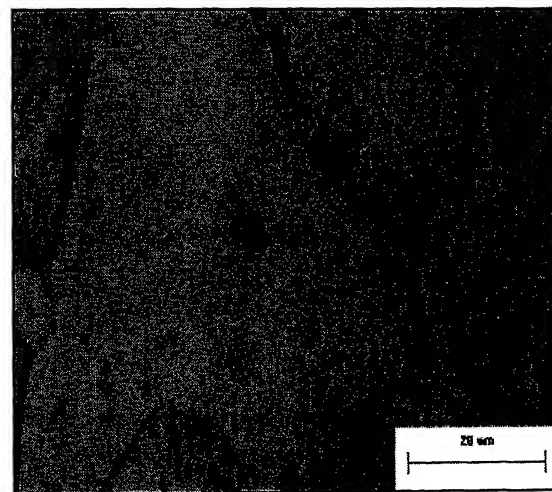
The recrystallization behaviour of the laminate composite was studied below the  $\beta$ -transus temperature (at  $650^0\text{C}$ ,  $700^0\text{C}$  and  $750^0\text{C}$  respectively) and also above the  $\beta$ -transus temperature (at  $800^0\text{C}$ ) of the metallic phase for varying time intervals. Figure 4.4(a) – (d) shows the microstructures of the composite in the region of metallic layers after an annealing treatment of 30 minutes at In order to get a fine structure of  $\beta$  phase samples were annealed for 30 minutes at  $650^0\text{C}$ ,  $700^0\text{C}$ ,  $750^0\text{C}$  and  $800^0\text{C}$  respectively. Microstructures obtained at these conditions indicate that there is not much change in the microstructure and the grain structure of the metallic phase remains more or less same after the short annealing time of 30 minutes.

In order to see the effect of annealing time on the recrystallization behaviour of the metallic phase in the laminate composite the material was also heated at  $700^0\text{C}$  for time intervals of 70 minutes, 12 hours, and 30 hours. Figure 4.5(a) – (c) show the microstructures obtained after these treatments. Though the annealing temperature is below the  $\beta$ -transus temperature, the precipitation of the  $\alpha$  phase does not appear to be occurring after even these long time intervals.

In order to study the precipitation of the  $\alpha$  phase in the laminate composite hot rolled at  $950^0\text{C}$ , another specimen of the material was heated at  $600^0\text{C}$  for 45 hours. Figure 4.6 shows the microstructure of the metallic phase layer after such a treatment. The precipitation of the  $\alpha$  phase is revealed in the structure. The precipitate size, however, was not fine implying that grain growth had taken place during this long time annealing treatment.



(a)



(b)

Fig 4.2 a-b Microstructures of (a) aluminide phase and (b)  $\beta$  alloy phase hot rolled at  $950^{\circ}\text{C}$  (500X)

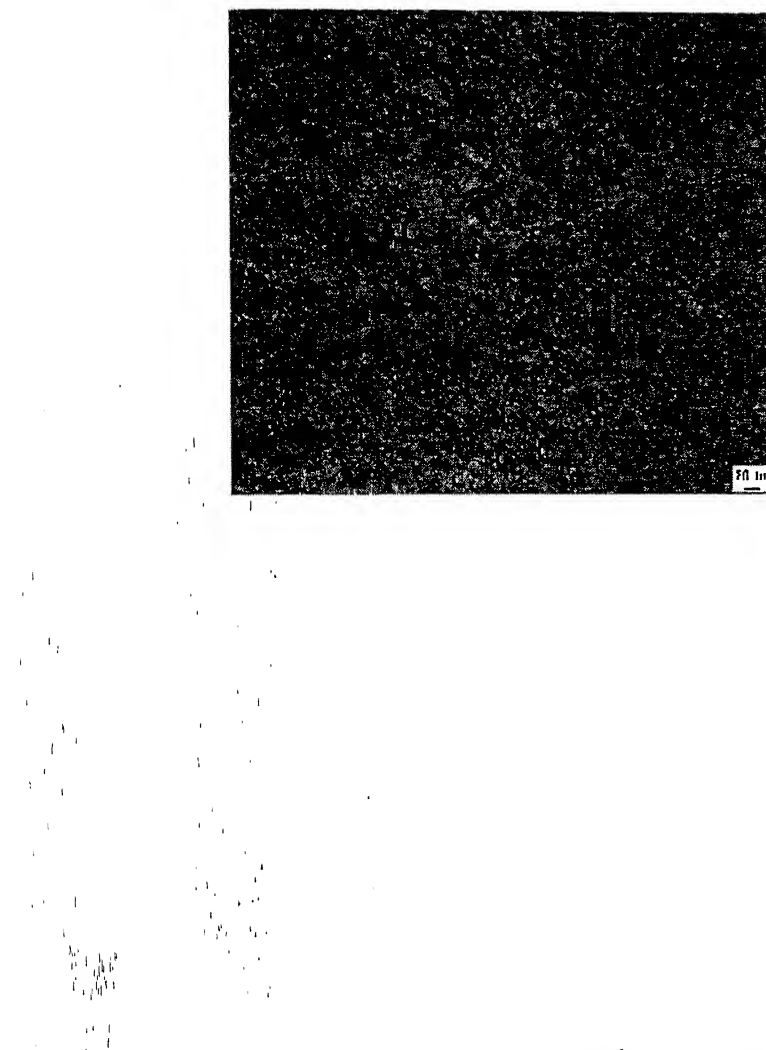
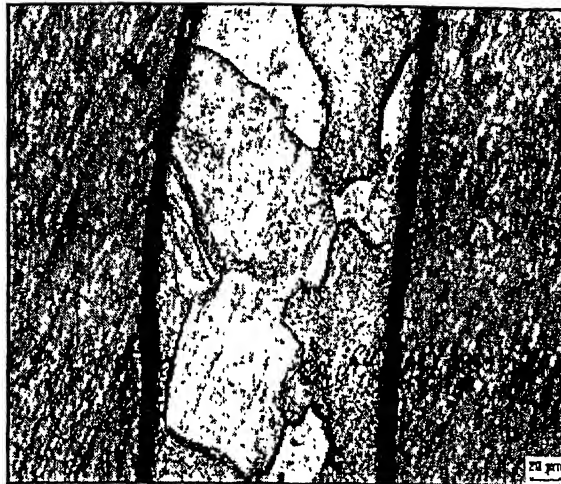


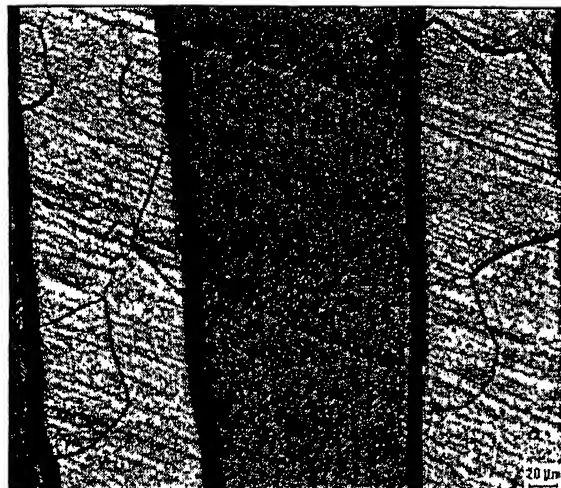
Figure 4.3 Microstructure of sample hot rolled at  $1000^{\circ}\text{C}$  and subsequently warm rolled at  $700^{\circ}\text{C}$  (500X)



(a)



(b)



(c)



(d)

Fig 4.4 a-d Microstructures of the sample hot rolled at  $950^0\text{C}$  and annealed for 30 minutes at (a)  $650^0\text{C}$  (b)  $750^0\text{C}$  (c)  $750^0\text{C}$  and (d)  $800^0\text{C}$ . Mag: 100X



(a)  
(Mag. 100X)



(b)  
(Mag. 200X)



(c)  
(Mag. 100X)

Fig 4.5 a-c Sample hot rolled at  $950^0\text{C}$  and annealed at  $700^0\text{C}$  for (a) 70 min (b) 20 hrs  
(c) 30 hrs



**Fig 4.6** Sample hot rolled at  $950^{\circ}\text{C}$  and annealed at  $650^{\circ}\text{C}$  for 45 hrs (200X)

#### 4.2.2 Annealing of Composite Material Rolled at 1000<sup>0</sup>C

Material hot- rolled at 1000 <sup>0</sup>C was annealed at 650 <sup>0</sup>C, 700 <sup>0</sup>C, 750 <sup>0</sup>C and 800<sup>0</sup>C respectively for the time interval of 30 minutes. As in the case of the composite rolled at 950<sup>0</sup>C, the structure obtained revealed almost no change in the  $\beta$  phase layer of the laminate. (Figure 4.7 (a)-(d)). This means that at this combination of annealing temperature and time there is no precipitation of the alpha phase in the material.

Another piece of the composite, initially hot rolled at 1000<sup>0</sup>C and subsequently warm rolled at 700<sup>0</sup>C (in the  $\alpha + \beta$  range) from the thickness of 2.3 mm to the thickness of 1.4 mm (about 39 % reduction). Specimens obtained from the warm rolled material were annealed at 700 <sup>0</sup>C for 2 hours and 24 hours respectively. Microstructures of these annealed samples are shown in Figure 4.8(a) and (b), and were still having coarse beta grains as in earlier cases (Fig 4.8 a-b).

Other pieces of the sample hot rolled at 1000<sup>0</sup>C and warm rolled at 700<sup>0</sup>C were annealed at 550 <sup>0</sup>C for 24 hours, 48 hours and 72 hours. Microstructures of the samples are shown in Figure 4.9 (a)-(c). Microstructure of these annealed samples revealed that very fine equiaxed grains precipitated in the metallic layer of the laminate composite which become coarser as annealing time increases.



(a)



(b)



(c)



(d)

Fig 4.7 a-d Sample hot rolled at  $1000^0\text{C}$  and annealed for 30 minutes for (a)  $650^0\text{C}$   
(b)  $700^0\text{C}$  (c)  $750^0\text{C}$  (d)  $800^0\text{C}$ . Mag: 100X

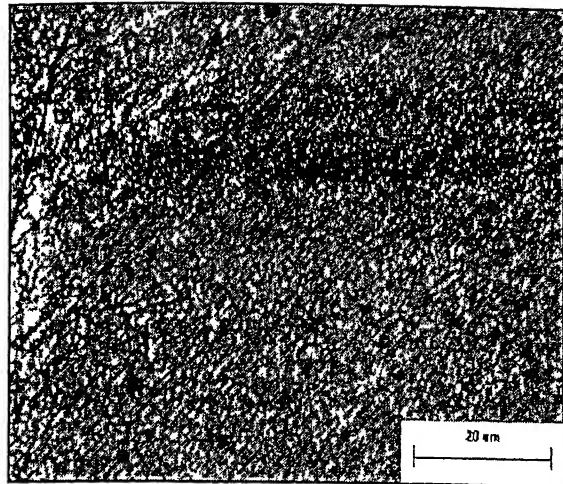


(a)

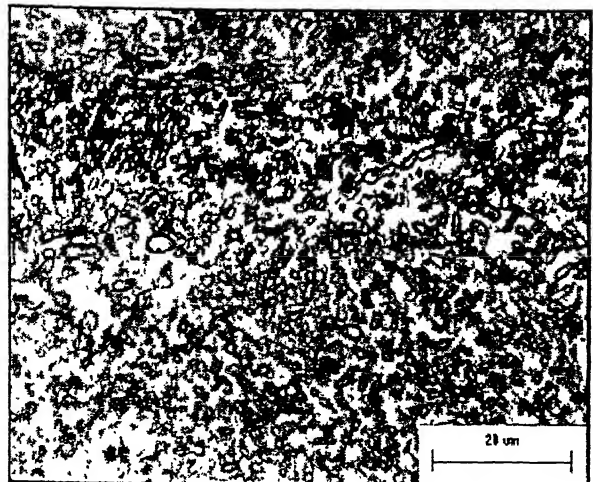


(b)

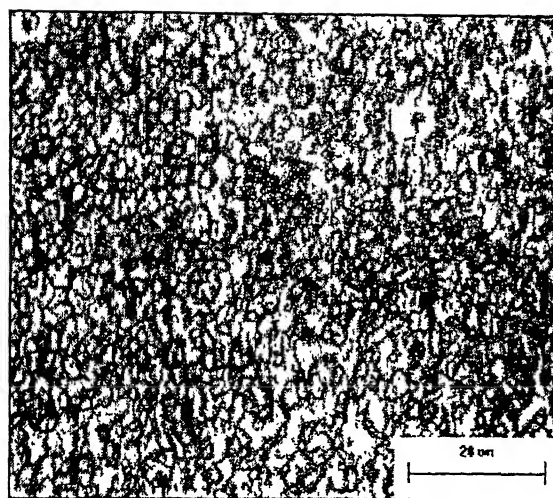
Fig 4.8 a-b Sample hot rolled at  $1000^0\text{C}$  / warm rolled at  $700^0\text{C}$  and annealed at  $700^0\text{C}$  for (a) 2 hrs (b) 20 hrs. Mag: 100



(a)



(b)



(c)

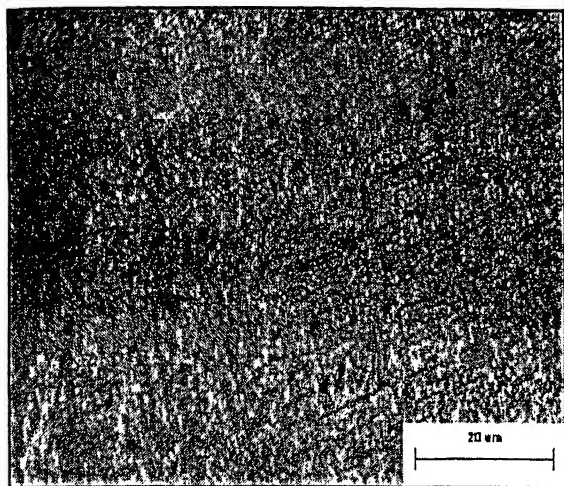
Fig 4.9 a-c Microstructures of sample hot rolled at  $1000^{\circ}\text{C}$  and warm rolled at  $700^{\circ}\text{C}$  and annealed at  $550^{\circ}\text{C}$  for (a) 24 hrs (b) 48 hrs (c) 72 hrs respectively.  
Mag: 500X.

#### 4.2.3 Material rolled at 1050 $^{\circ}\text{C}$ .

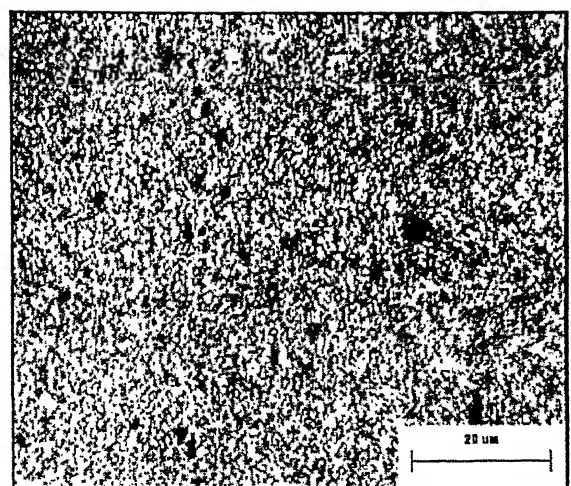
The microstructural development of earlier thermomechanical processing and annealing response suggested that optimum temperature to get a very fine recrystallized grains of beta phase is about 550  $^{\circ}\text{C}$  with sufficient time for the nucleation of fine beta grains.

Microstructure of the sample rolled at this temperature and annealed at 550  $^{\circ}\text{C}$  for 3 hrs suggests that nucleation of the beta phase grains is not completed although some grains might have nucleated (Fig 4.10(a)-(c)), more details about it can only be found with back scattered photographs with Scanning Electron Microscope (SEM).

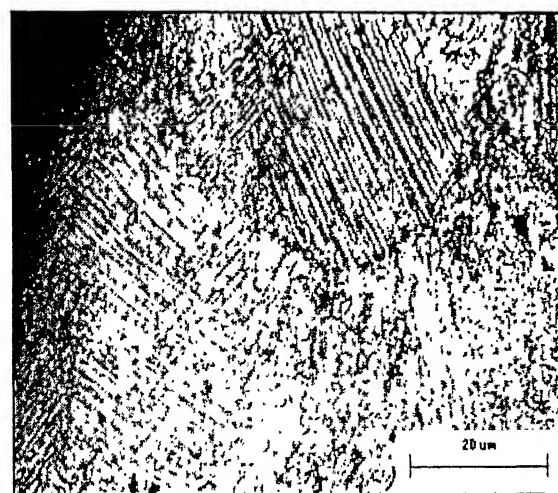
Microstructures of the sample annealed at 550  $^{\circ}\text{C}$  for 12 hrs, 18 hrs, 24 hrs, 48 hrs and 72 hrs (fig 4.11(a)-(c)) indicated that very fine grains in pancakes form are nucleated with these combination of temperatures. Quantitative microscopy of these microstructures showed that as annealing time increases, the grain size also increases. Compared to grains nucleated in case of sample hot rolled at 1000 $^{\circ}\text{C}$  and warm rolled 700 $^{\circ}\text{C}$  with same annealing time, in the present case grains are more elongated in rolling direction. Aspect ratio of the grains also increases as annealing time increases (Table 4.1 and Fig 4.12); this indicates that preferred direction of grain growth is along the direction of rolling.



(a)

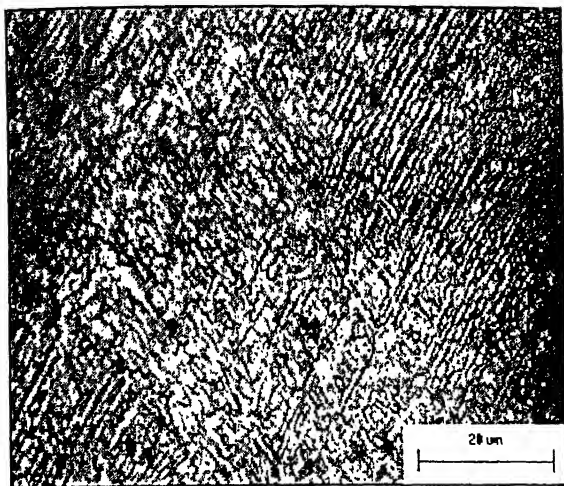


(b)

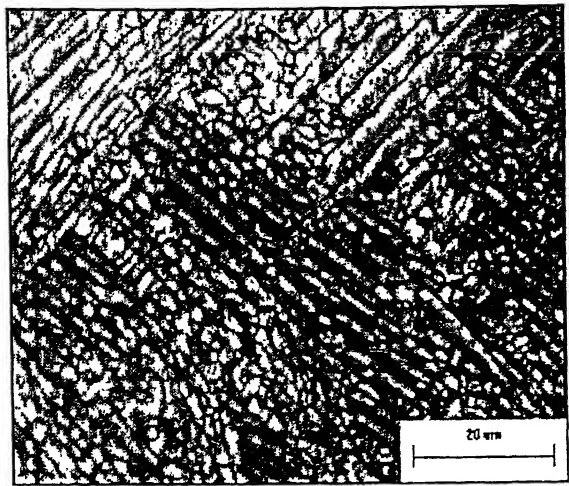


(c)

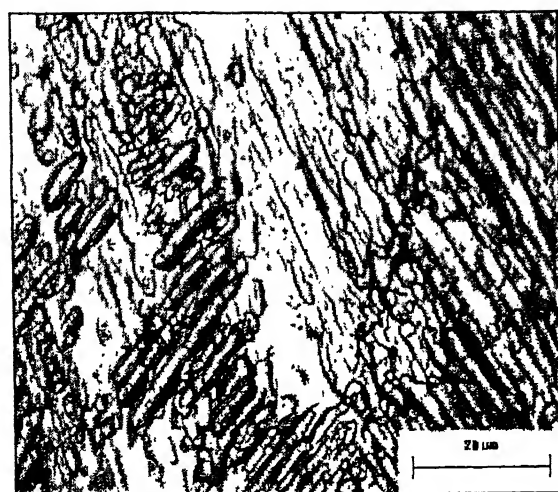
Fig 4.10 a-c Microstructures of the sample hot rolled at  $1050^0\text{C}$  and annealed at  $550^0\text{C}$  for  
(a) 3 hrs (b) 12 hrs (c) 18 hrs. Mag: 500X



(a)



(b)



(c)

Fig 4.11 a-c Microstructures of the sample hot rolled at  $1050^0\text{C}$  and annealed at  $550^0\text{C}$  for  
(a)24 hrs (b) 48 hrs (c) 72 hrs. Mag: 500X

Table 4.1 Grain size as a function of annealing time for the sample hot rolled at  $1050^0\text{C}$  and annealed at  $550^0\text{C}$

Annealing time (hrs)	Grain size (microns)
12	3.36
18	5.21
24	5.32
48	10.55
72	11.90

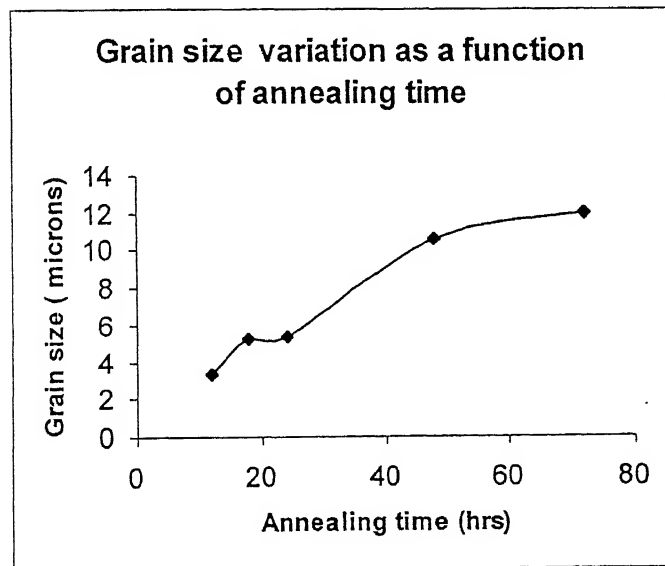


Fig 4.12 Grain size vs. Annealing time curve

पुस्तकालय  
भारतीय वाणिज्यकी संस्थान कानपुर

अंकाप्ति क्र. A-141916

Table 4.2 Aspect ratio as a function of annealing time for the sample hot rolled at  $1050^{\circ}\text{C}$  and annealed at  $550^{\circ}\text{C}$

Annealing time (hrs)	Aspect ratio
12	1.69
18	1.73
24	1.88
48	2.4
72	2.425

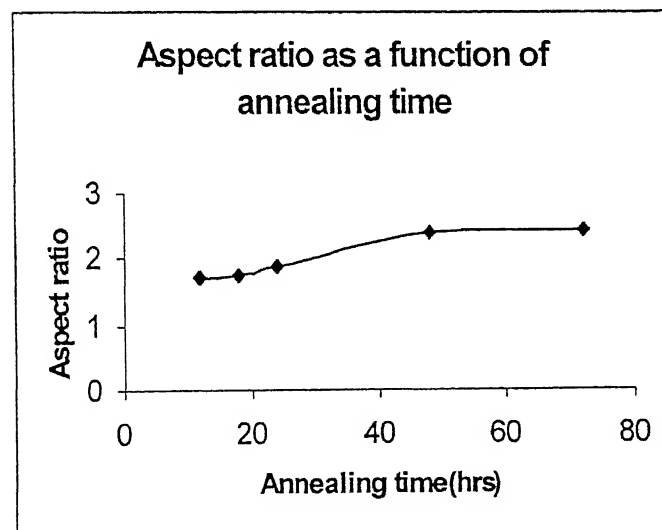


Fig 4.13 Aspect ratio vs. Annealing time curve

## 4.3 Mechanical Behavior of Thermomechanically Treated Laminate Composites

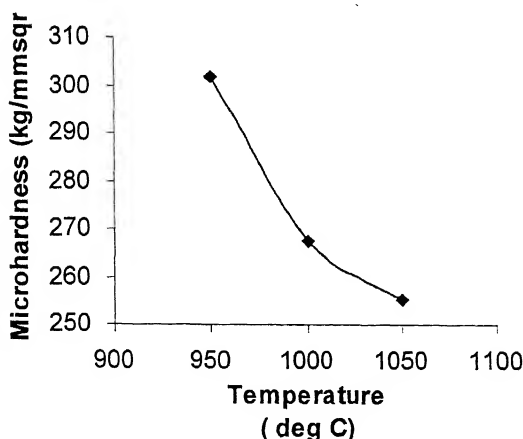
### 4.3.1 Effect of Thermomechanical / Annealing Treatment on the Microhardness of $\beta$ and Aluminide layers

Microhardness values of the samples after different thermomechanical treatments and annealing at different temperatures / times were measured using Leitz Miniload Microhardness Tester under different loads. For each layer of the composite four to twelve readings of the diagonal of indentation were taken and from these values average value was calculated using the formula.

$$VHN = 1854.4 * P(\text{in gm}) / d^2(\text{in } \mu\text{m})$$

The as-received Hot Pressed Laminate Composite had the microhardness value (VHN) of aluminide layer as  $275.31 \text{ kg/mm}^2$  and  $262.36 \text{ kg/mm}^2$  for the  $\beta$ -titanium alloy layer. The microhardness values of the laminate composite after hot rolling at three different temperatures (i.e.  $950^0\text{C}$ ,  $1000^0\text{C}$  and  $1050^0\text{C}$ ) indicated that as the rolling temperature increased, the microhardness value decreased for both the layers of the composite. For the rolling temperature of  $950^0\text{C}$  the microhardness value of the titanium aluminide phase increases which is due to mechanical working of the material below  $\beta$  transus temperature of the (O+ B-2) phase of the laminate composite, however, microhardness value of the  $\beta$  titanium alloy layer goes down, this is attributed to the grain coarsening of this layer as material is soaked for 30 minutes prior to rolling and at this temperature (above the  $\beta$  transus temperature for the  $\beta$  titanium alloy layer) rapid grain coarsening took place in the  $\beta$ -Alloy layer. As the rolling temperature increases the microhardness value of the both the layer goes down as softening takes place due to soaking at high temperature (Fig 4.14 and 4.15c).

**Microhardness value of Aluminide layer with different rolling temperature**



**Microhardness variation of beta layer with different rolling temperatures**

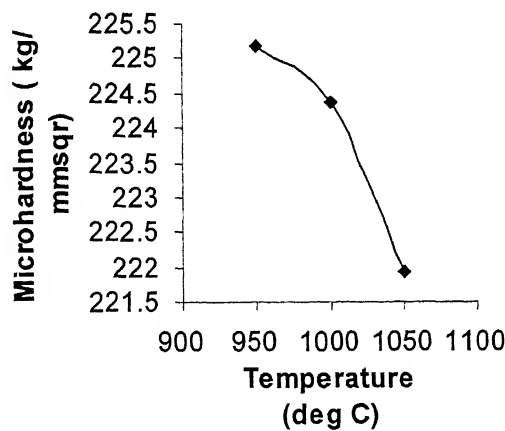


**Fig 4.14** Microhardness values of (a) aluminide layer and (b)  $\square$  -titanium Alloy layer as the function of rolling temperature

Table 4.3 Microhardness values for the two layers at different rolling temperatures

Temperature of rolling (in $^{\circ}\text{C}$ )	Microhardness of aluminide layer of the composite in $(\text{kg}/\text{mm}^2)$	Microhardness of $\beta$ layer of composite in $(\text{kg}/\text{mm}^2)$
950	301.69	225.19
1000	267.64	224.37
1050	255.22	221.92

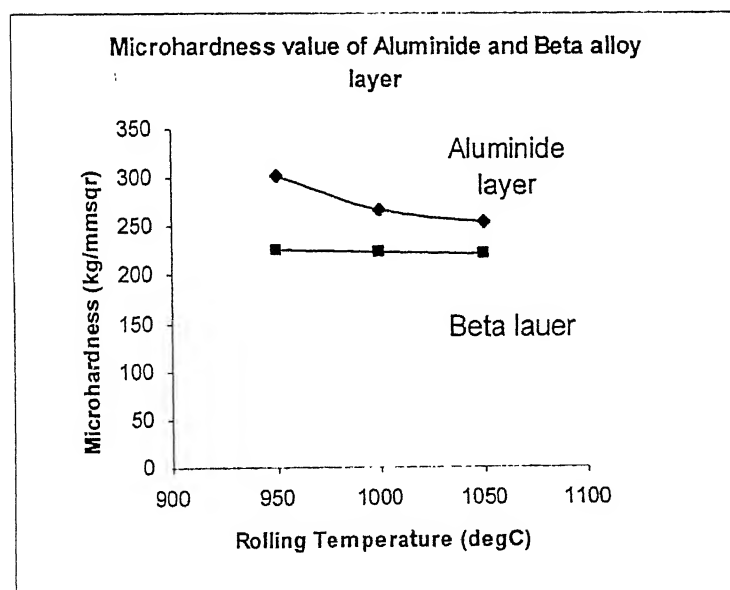
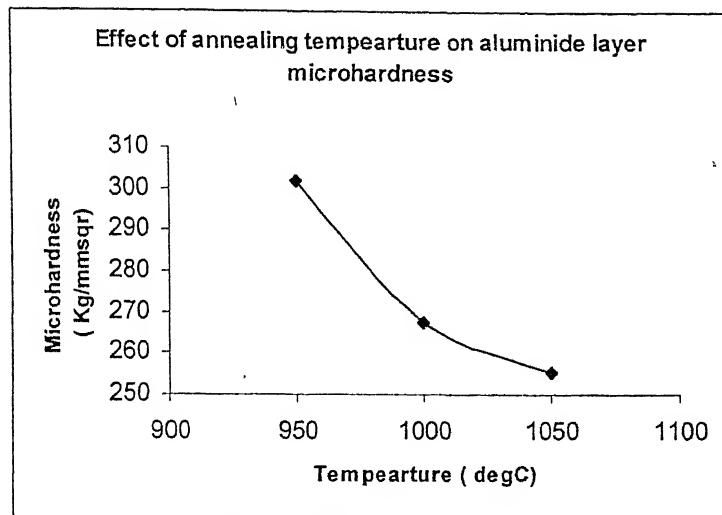
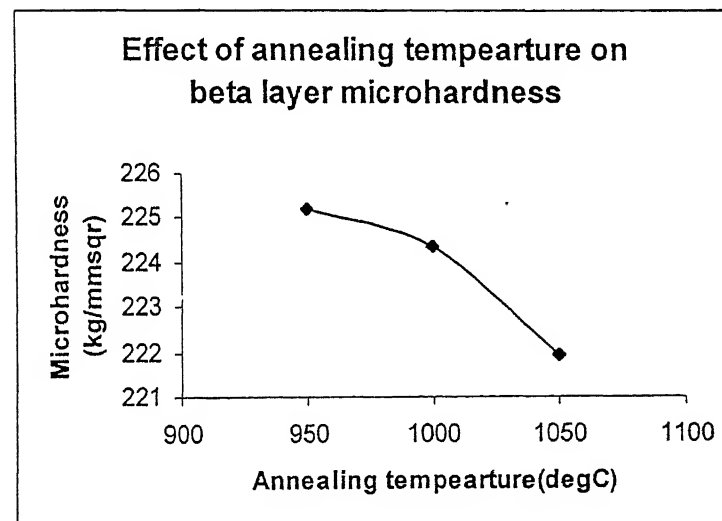


Fig 4.15 Microhardness value as a function of rolling temperature



(a)



(b)

Fig 4.16 Microhardness value as a function of annealing temperature for  
(a) aluminide layer  
(b)  $\beta$  Alloy layer

Table 4.4 Microhardness values for the two layers as a function of annealing temperatures

Annealing temperature (deg C)	Microhardness of aluminide layer of composite (kg /mm <sup>2</sup> )	Microhardness of beta layer of composite (kg /mm <sup>2</sup> )
650	249.3	227.91
700	236.12	220.12
750	199	183.64
800	192.63	175.26

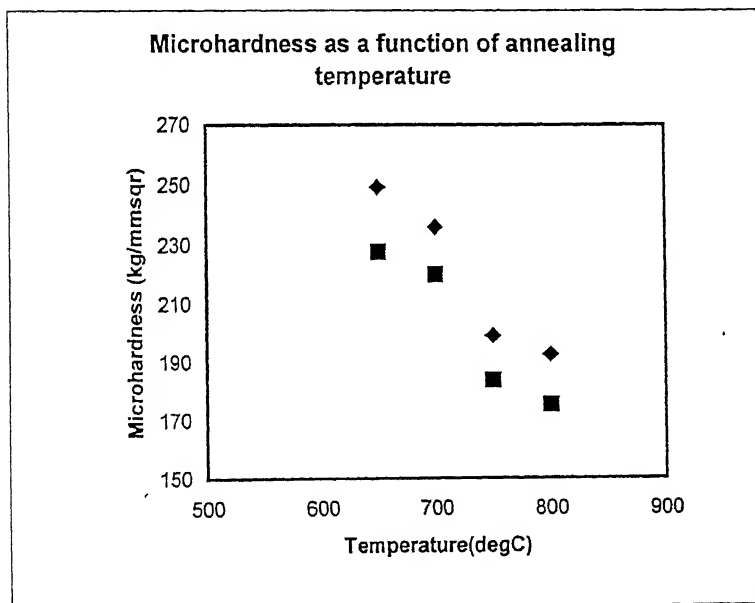
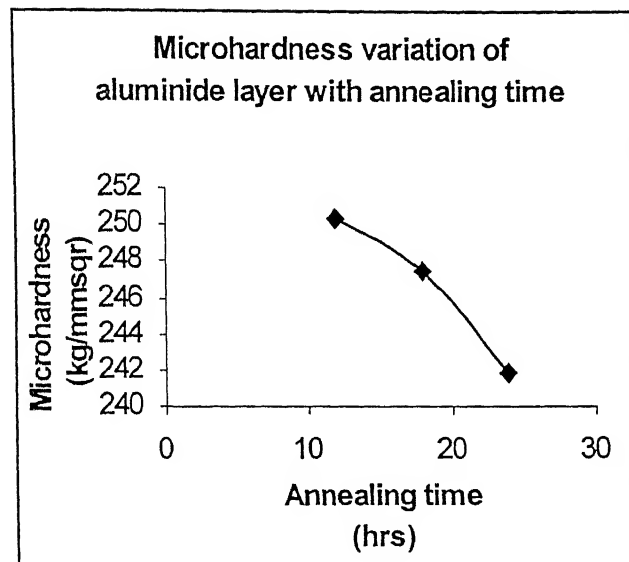
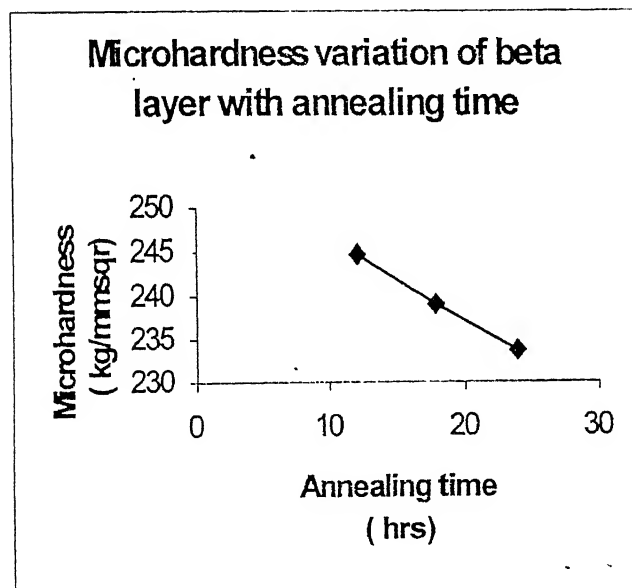


Fig 4.17 Microhardness value as a function of annealing temperature.



(a)



(b)

Fig 4.18 a-b Microhardness value as a function of annealing time

(a) Aluminide Layer

(b)  $\beta$  alloy layer

Table 4.5 Microhardness behavior of composite with annealing time

Annealing time (hrs)	Microhardness of aluminide layer of composite (kg /mm <sup>2</sup> )	Microhardness of beta layer of composite in (kg /mm <sup>2</sup> )
12	250.3	244.58
18	247.4	239
24	241.8	233.71

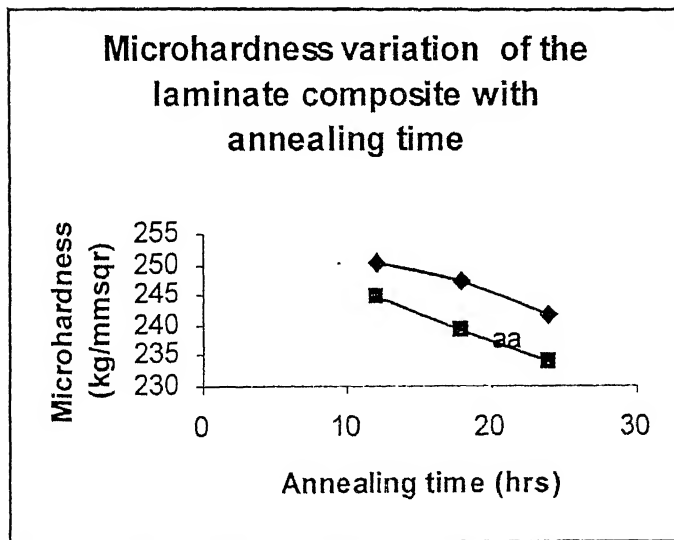


Fig 4.19 Microhardness value as a function of annealing time

## 4.3.2 Tensile Behavior of Thermomechanically treated Laminate Composite

### 4.3.2.1 Tensile Behavior at High Temperature

In order to study the high temperature tensile properties of the composite, samples rolled at  $1050^0$  and  $1000^0$  were tested at temperatures  $800^0\text{C}$  and  $700^0\text{C}$  respectively. The values of the YS, UTS and % elongation of the samples tested at the two temperature are given in Table 4.6. As % elongation of the sample (LC3) tested at  $800^0\text{C}$  was 28 % and that for sample tested at  $700^0$  was 20.8 %, these results indicate that the hot rolled laminate composite has a reasonably good ductility in the range of the testing temperature. However, the material flow at these temperatures was found to have very low values of the strain rate sensitivity and hence did not display any superplastic behaviour at these temperatures. The results of the high temperature tensile testing also show that as the testing temperature increases, the yield strength (YS) and the ultimate tensile strength (UTS) go down.

### 4.3.2.1 Tensile Behavior at Room Temperature

Samples hot rolled at  $1050^0\text{C}$  and  $1000^0\text{C}$  and  $950^0\text{C}$  were tested at room temperature. The results of the tensile testing experiments reveal that sample rolled at higher temperature ( $1050^0\text{C}$ ) had more ductility but lower YS and UTS compared to sample rolled at lower temperatures (e.g.  $1000^0\text{C}$  and  $950^0\text{C}$ ) (Table 4.7 and Figure 4.18, 4.19).

Results of the tensile testing of the samples rolled at  $1000^0\text{C}$  and  $950^0\text{C}$  and annealed at  $550^0\text{C}$  for 24 hrs shows that annealed samples have higher strength but lower percentage elongation and toughness. This is attributed to formation of relatively brittle  $\alpha$  phase during annealing (Table 4.8). Further, sample hot rolled at  $1000^0\text{C}$  and warm rolled at  $700^0\text{C}$  (LC2a) after annealing shows very low strength, ductility and toughness (Table 4.9). This is again due to formation of a higher volume fraction of more brittle  $\alpha$  phase in the  $\beta$  alloy layer. Though fractographic analysis of the broken tensile pieces could not be done,

lower values of strength also indicate that there is finite chance of interface delamination of the sample due to warm rolling.

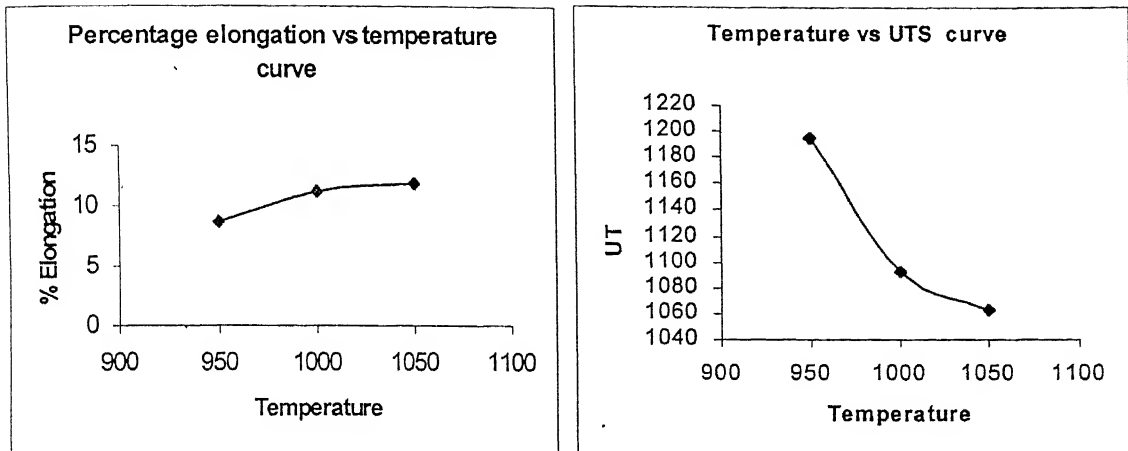
Results of tensile properties obtained in the present study are now compared with those obtained on several  $\beta$  titanium alloys, titanium aluminide and the laminate composite produced by Satyam Suwas et al.[3]. Tensile properties of  $\beta$  titanium alloys, titanium aluminide and their laminate composites have been summarized in Table 4.10 (a)-(c).

Table 4.6 Strength and Elongation in the sample tested at higher temperature

Sample/Temp( $^{\circ}$ C)	YS (MPa)	UTS (MPa)	%Elongation
LC3 at 800 $^{\circ}$ C	116	151	28.0
LC2 at 700 $^{\circ}$ C	388	446	20.8

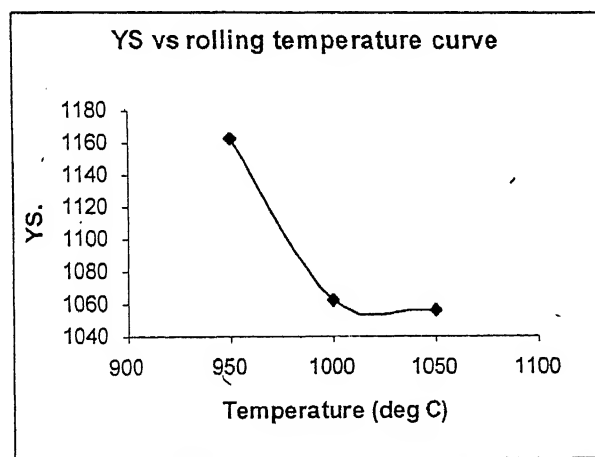
Table 4.7 Yield Strength, UTS and Percentage Elongation (at room temperature) of the samples rolled at three different temperatures.

Rolling condition	YS (MPa)	UTS (MPa)	%Elongation
Rolled at 950 $^{\circ}$ C	1163	1194	8.62
Rolled at 1000 $^{\circ}$ C	1062	1093	11.12
Rolled at 1050 $^{\circ}$ C	1056	1062	11.81



(a)

(b)



(c)

Fig 4.21 a-c Room temperature tensile properties for three rolling temperatures  
 (a)% Elongation (b)UTS (c) YS.

**Table 4.8 YS, UTS and Percentage Elongation of the samples rolled at three different temperatures and annealed at 550 deg C for 24 hrs**

<b>Rolling condition</b>	<b>YS (MPa)</b>	<b>UTS (MPa)</b>	<b>% Elongation</b>
Rolled at 950 $^{\circ}\text{C}$	1012	1269	3.25
Rolled at 1000 $^{\circ}\text{C}$	956	1180	3.75

**Table 4.9 Tensile properties of sample hot rolled at 1000  $^{\circ}\text{C}$ , warm rolled at 700  $^{\circ}\text{C}$  and annealed at 550  $^{\circ}\text{C}$  for 24 hours**

<b>Sample</b>	<b>YS</b>	<b>UTS(MPa)</b>	<b>% Elongation</b>
LC2a	*	670	3.1

- Could not be taken due to slipping of sample.

Table 4.10(a) Mechanical properties of some Ti based intermetallics

Alloy	YS (Mpa)	UTS (Mpa)	% Elongation
Ti-24Al-11Nb	787	824	0.7
Ti-24Al-14Nb	831	977	2.1
Ti-25Al-10Nb-3V-1Mo	825	1042	2.2
Ti-24.5Al-17Nb	952	1097	2.7
Ti-25Al-17Nb-1Mo	989	1133	3.4

Table 4.10(b) Mechanical properties of some  $\beta$  Titanium alloys

Alloy	YS (Mpa)	UTS( Mpa)	%Elongation
Ti-10V-2Fe-3Al	1100-1200	1170-1276	10
Ti-13V-11Cr-3Al	1100-1172	1170-1220	8

Table 4.10(c) Mechanical properties of 12 layered hot pressed Ti-aluminide (O+B2) and  $\beta$  Titanium alloy hot rolled to 2 mm thick sheet [3]

Processing condition	YS (Mpa)	UTS (Mpa)	%Elongation
1060 $^{\circ}$ C (WQ)	784	819	11.9
1060 $^{\circ}$ C (WQ) $\rightarrow$ 650 $^{\circ}$ C(24hrs)	1136	1147	0.24
1060 $^{\circ}$ C (FC)	1245	1311	1.39

# Chapter 5

## CONCLUSIONS

Some major conclusions that have been resulted from the present investigations are

- 1 Hot rolling behaviour of the laminate composite at the rolling temperatures of  $950^0\text{C}$ ,  $1000^0\text{C}$  and  $1050^0\text{C}$  (all the temperatures being above the  $\beta$ -transus temperature of the metallic phase and below the transus temperature of the intermetallic phase) shows that the material could be hot rolled up to about 10% to 15% thickness reduction in a single pass without any edge and/or surface cracking. Microstructures of hot rolled samples show elongated  $\beta$  grains in the metallic phase indicating that no dynamic recrystallization takes place in metallic phase. In contrast, the intermetallic phase shows the presence of fine equiaxed grains.
- 2 Warm rolling at  $700^0\text{C}$ , i.e. below the  $\beta$ -transus temperature of the metallic phase, can be done with low values of % thickness reduction in a single pass. Laminate composites were subjected to about 39% thickness reduction in 7-8 passes by warm rolling.
- 3 Annealing behaviour of the laminate composite shows that annealing above  $\beta$  transus of the  $\beta$  alloy results into coarse  $\beta$  grains in the metallic phase. In contrast, annealing at temperatures below the  $\beta$  transus of the metallic phase, i.e. at  $550^0\text{C}$ ,  $600^0\text{C}$ ,  $650^0\text{C}$  and  $700^0\text{C}$ , for sufficiently long time intervals results in the precipitation of fine  $\alpha$  grains in  $\beta$  alloy layer of the composite.
- 4 Room temperature tensile testing of the hot rolled titanium alloy – titanium aluminide composite shows that the tensile properties of the laminate composite depends on the hot rolling temperature. For the samples rolled at  $950^0\text{C}$ , the yield strength has been found to be  $> 1150$  MPa which is roughly equal to that predicted by the rule of mixtures for the laminate composites. UTS of the

composite rolled at this temperature is found to be  $>1190$  MPa. The composite is also more ductile, having about 9% elongation, than that reported in the literature.

- 5 While the yield strength and the UTS of the laminate composite deteriorate when the hot rolling temperature is increased above  $950^0\text{C}$ , the ductility increases. Values of about 1060 MPa and 1050 MPa for the yield strength and 1090 MPa and 1060 MPa for the UTS were obtained for the laminate composites rolled at  $1000^0\text{C}$  and  $1050^0\text{C}$  respectively. The ductility in both the cases was about 11 % elongation.
- 6 An annealing treatment of 24 hours at  $550^0\text{C}$  deteriorates the yield strength as well as the ductility of the laminate composite rolled at  $950^0\text{C}$  and  $1000^0\text{C}$ . However, this treatment increases the ultimate tensile strength of the material.
- 7 Laminate composites subjected to warm rolling at temperatures below the  $\beta$ -transus temperature of the metallic phase display inferior tensile properties. Warm rolling of the laminate composites therefore is not recommended.
- 8 Laminate composite loses its strength as the temperature of testing increases. Composite shows the yield strength of about 380 MPa 115 MPa and UTS of 445 MPa and 150 MPa at  $700^0\text{C}$  and  $800^0\text{C}$  respectively.

### ***SUGGESTIONS FOR FUTURE WORK***

1. Laminates with smaller layer thickness could be tried for better mechanical properties.
2. Scanning electron microscope and transmission electron microscope should be used for the detailed study of fracture surface and microstructural study of the composite especially Aluminide phase.

## REFERENCES

1. M.Blanck-Bewersdorff and J.A. Peters, *Scripta Metallurgica* V 31, No.7 (1994),pp945.
2. S.Krishnamurthy, P.R.Smith, and D.B.Miracle, *Scripta Metallurgica*, V 31, No.6(1994), pp653.
3. Satyam Suwas, T.K.Nandy, V.V.Bhanu Prasad, S.V.Kamat and D. Banerjee, *DMRL Hyderabad, personal communication.*
4. H.T.Weykamp, D.R.Baker, D.M.Paxton, and M.J.Kaufman, *Scripta Metallurgica*, V 24(1990), pp445.
5. M.J. Donachie, Jr., in *Titanium and Titanium Alloys: A Source book*, ASM, (1982).
6. S.R.Seagle and L.J.Barillo, in *Titanium and Titanium Alloys: A Source Book*, ASM, (1982).
7. Molchanova, E.K., *Phase Diagrams of Ti alloys*, Israel Program for Scientific Translations, 1965.
8. Zwicker. U, *Titan and Titanlegierungen*, Springer Verlag, 1974.
9. Rosenberg H.W., *Titanium Alloying in Theory and Practice in the Sci. Tech and Application of Titanium* ( Proc first Int. Conferenceon Titanium, London, R.I.Jaffee and N.E. Promisel, Ed.,Pergamom Press, 1970, pp.851.
10. J.E.Gould, W.A. Balblact III, and J.C.Williams, in *Ad. Proc. Methods for Titanium*, Proc Conf. The Met. Soc. Of AMIE, TMS Fall, Kentucky, Oct 13-15, 1981, Ed. D.F.Harson and C.H.Hamilton, pp.203
11. Wood, R.A., *Titanium Alloys Handbook*, Metals and Ceramics Information Centre, Battelle, Pub. No. MCIC-HB-02, Dec. 1972.

12. Salomon D.R., Low Temperature Data Handbook, titanium and Titanium Alloys, National Physical Labs, NPL Report Q 453(N8023448), May 1979.
13. Smith, Structure and Properties of Engg. Alloys., pp 449.
14. Gorynin, I.V., Chechulin, B.B., Ushkov, S.S. and Belova, O.S., A study of the nature of the Ductile -Brittle Transition in Beta Titanium Alloys, in Titanium Sci and Tech. ( Proc. Second Int. Conf. on Titanium Boston, Eds: Jaffee II and Brute, H.M. Plenum Press 1973).
15. H.M. Flower, P.R. Swann and D.R.F. West, Met. Trans., Vol 2, (1971) pp. 3289.
16. W.J. Plumbridge and M Stanley, Int. J. Fatigue, 1986, Vol 8, pp 209.
17. Microstructural Standards for  $\alpha+\beta$  Titanium Alloy Bars, Prepared by The Technical Committee of European Titanium Producers, 1979.
18. W.A. Reinsch ; Terminology for Titanium Microstructures, "Metal Progress", Vol 121, No.2, Feb 1982, pp51.
19. G. Welsch, R. Boyer ; Technical Note 1: Metallography and Microstructure, pp1051.
20. G.E. Dieter, in: *Mechanical Metallurgy*, McGraw Hill, (1988), 283.
21. D.R. Lesuer, C.K. Syn, O.D. Sherby, J. Wadsworth, J.J. Lewandowski, and W.H. Hunt, Jr, International Materials Review 1996 Vol 41, No 5 pp 169.